Supplementary Materials

Construction of a novel tetraphenylethylene-based supramolecular dimer for improving the generation of reactive oxygen species and photocatalytic performance

Man Jiang[1,#], Xin-Long Li[2,#], Ning Han[2], Xian-Ya Yao[2], Fa-Dong Wang[2], Kai-Kai Niu[2], Hui Liu[2], Shengsheng Yu[2], Ling-Bao Xing[2,*]

[1]School of Resources and Environmental Engineering, Shandong University of Technology, Zibo 255000, Shandong, China.
[2]School of Chemistry and Chemical Engineering, Shandong University of Technology, Zibo 255000, Shandong, China.
[#]Authors contributed equally.

[*]**Correspondence to:** Prof. Ling-Bao Xing, School of Chemistry and Chemical Engineering, Shandong University of Technology, 266 Xincun West Road, Zhangdian District, Zibo 255000, Shandong, China. E-mail: lbxing@sdut.edu.cn

Table of contents

1. Detection of ROS production in solution

Compound 2,7-Dichlorodihydrofluorescein diacetate (DCFH-DA) was used as an indicator for detection of ROS in solution (Figure 5).[1] 20 μM of photocatalyst was dissolved in 3.0 mL solution containing 20 μM of DCFH-DA. The mixture was then placed in a cuvette and irradiated with a purple light (400 nm). The fluorescence emission change of the sample at 525 nm was recorded by the fluorescence emission spectra. The excitation wavelength was 485 nm.

2. Detection of $^1O_2$ production in solution

Compound 9,10-anthracenediyl-bis(methylene)-dimalonic acid (ABDA) was used as an indicator for detection of $^1O_2$ in solution (Figure 6). 20 μM of photocatalyst was dissolved in 3.0 mL solution containing 50 μM of ABDA. The mixture was then placed in a cuvette and irradiated with a purple light (400 nm). The absorption change of the sample at 378 nm was recorded by the UV-vis absorption spectrophotometer.

3. Detection of $O_2^{\bullet-}$ production in solution

Compound N, N, N', N'-Tetramethyl-p-phenylenediamine (TMPD) was used as an indicator for detection of $O_2^{\bullet-}$ in solution.[2] the 1.0 mM TMPD solution in DMSO was added to the aqueous solution to form a 100 μM solution. 20 μM photocatalyst was added into TMPD solution respectively for $O_2^{\bullet-}$ generation measurement. The mixture was then placed in a cuvette and irradiated with purple light (400 nm). The generation of $O_2^{\bullet-}$ was detected by monitoring the absorption at 563 nm and 612 nm through UV-vis absorption spectra.

4. General procedure for the EPR

Electron Paramagnetic Resonance (EPR) were characterized on Bruker EMXplus-6/1. 20 μM of photocatalyst was dissolved in 3.0 mL solution containing 100 μM of TEMP or DMPO. The mixed solution was then taken with a microsyringe and placed in the EPR tube and irradiated with a purple light (400 nm) for 30s. The signal was observed by the corresponding software.

5. Calculation of $^1O_2$ efficiency

The $^1O_2$ quantum yield was measured using Rose Bengal (RB) as the reference photosensitizer and calculated using the following:

$$\Phi_{probe} = \Phi_{RB} \times K_{probe} A_{RB} / K_{RB} A_{probe}$$

where K_{probe} and K_{RB} are the decomposition rate constants of ABDA in the presence of the probe and RB, respectively. Φ_{RB} is the $^1O_2$ quantum yield of RB ($\Phi_{RB} = 0.75$) in water). A_{probe} and A_{RB} represent the integration area of absorption bands ranging from 400-405 nm of the probe and RB, respectively. The 50 μM ABDA in 3.0 mL of the probe solution was exposed to green irradiation (500-505 nm) with a power density of 10 W. The natural logarithm of the absorbance ratio (A_0/A) of ABDA at 378 nm was plotted against irradiation time and the slope is regarded as the decomposition rate.

6. General procedure for the oxidation of phosphine

Phosphine substrates (0.2 mmol) were dissolved in the freshly prepared 2TPE-Py-I@CB[8] aqueous solution (1.0 mol%, 2.0 mL). The mixture was subsequently irradiated by purple light (400 nm) at room temperature for 24 h. After that, it was extracted with dichloromethane, and the combined organic layer was dried with anhydrous Na_2SO_4. Then the organic solvent was concentrated in a vacuum. The crude product was separated by flash column chromatography with petroleum ether/ethyl acetate to obtain the product.

7. General procedure for the CDC reaction

2-phenyl-1,2,3,4-tetrahydroisoquinoline derivatives (0.1 mmol) and indole derivatives (0.2 mmol) were dissolved in the freshly prepared 2TPE-Py-I@CB[8] assembly solution (1.0 mol%, 2.0 mL). The mixture was subsequently irradiated by purple light (400 nm) at room temperature for 24 h. After that, it was extracted with dichloromethane, and the combined organic layer was dried with anhydrous Na_2SO_4. Then the organic solvent was concentrated in a vacuum. The crude product was separated by flash column chromatography with petroleum ether/ethyl acetate to obtain the product.

8. Synthetic route of TPE-Py-I

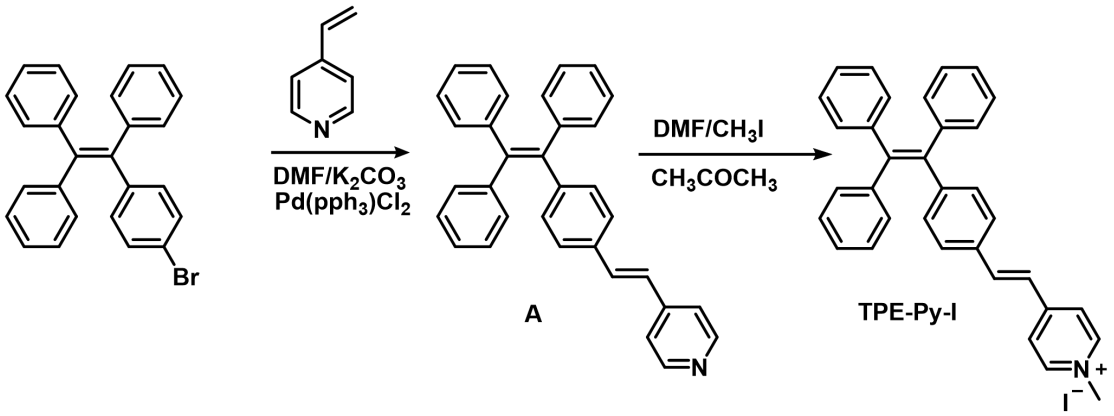

Supplementary Scheme 1. The synthetic route of the TPE-Py-I target molecule.

Synthetic of compound A[3]**:** (2-(4-bromophenyl)ethene-1,1,2-triyl)tribenzene (410 mg, 1.0 mmol), 4-vinylpyridine (105 mg, 1.0 mmol), $Pd(pph_3)_2Cl_2$ (70 mg ,0.1 mmol) and K_2CO_3 (690 mg, 5 mmol) were dissolved in 20 mL DMF and refluxed for 3 days. After cool to room temperature, extracted the organic phase with dichloromethane and concentrated it under vacuum. Then, the crude product was separated by flash column chromatography with petroleum ether/ethyl acetate = 5:1 to obtain a light yellow solid (350 mg, 0.80 mmol, 80%). ^{1}H NMR (400 MHz, DMSO-d_6) δ 8.54 - 8.51 (m, 2H), 7.54 - 7.51 (m, 2H), 7.46 - 7.41 (m, 3H), 7.18 - 7.12 (m, 10H), 7.02 - 6.97 (m, 8H).

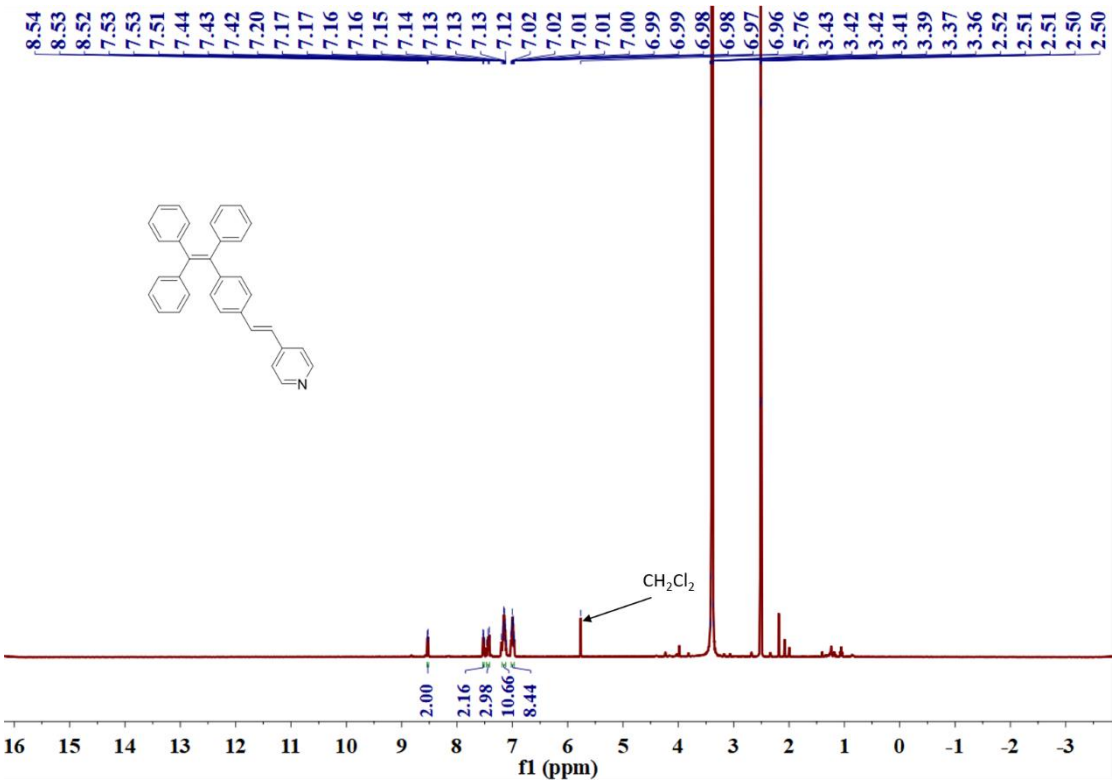

Supplementary Figure 1. ^{1}H NMR spectra of compound **A** in DMSO-d_6.

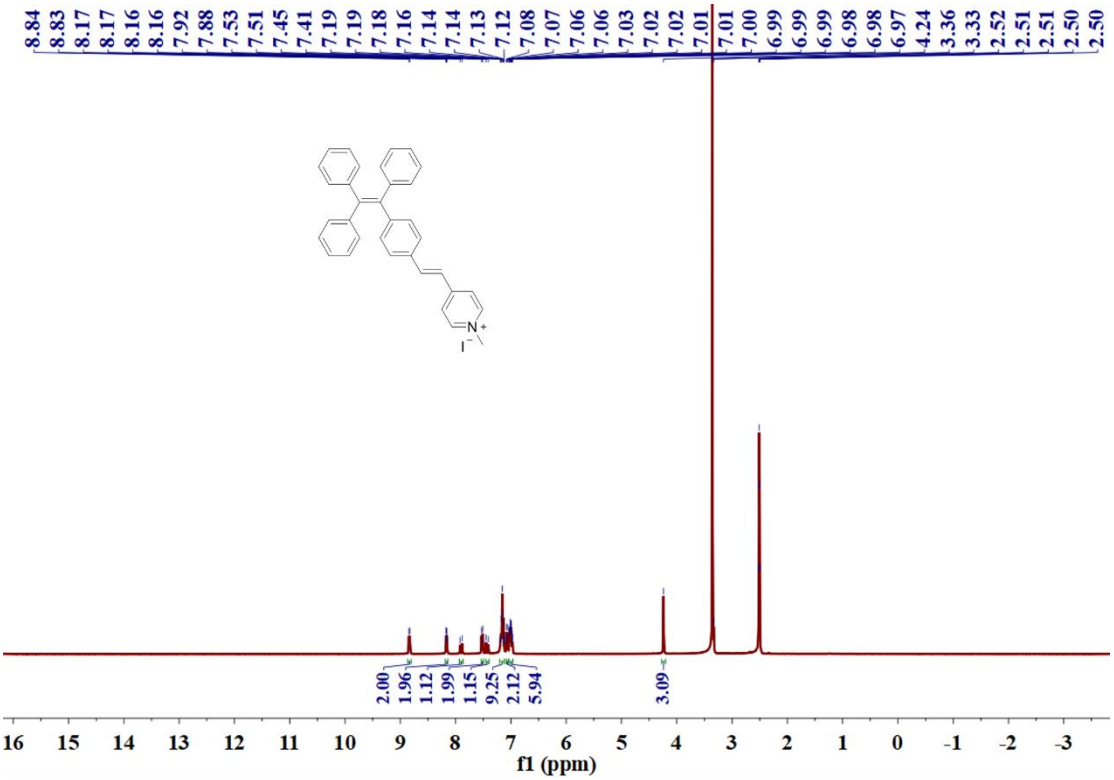

Supplementary Figure 2. ^{1}H NMR spectra of **TPE-Py-I** in DMSO-d_6.

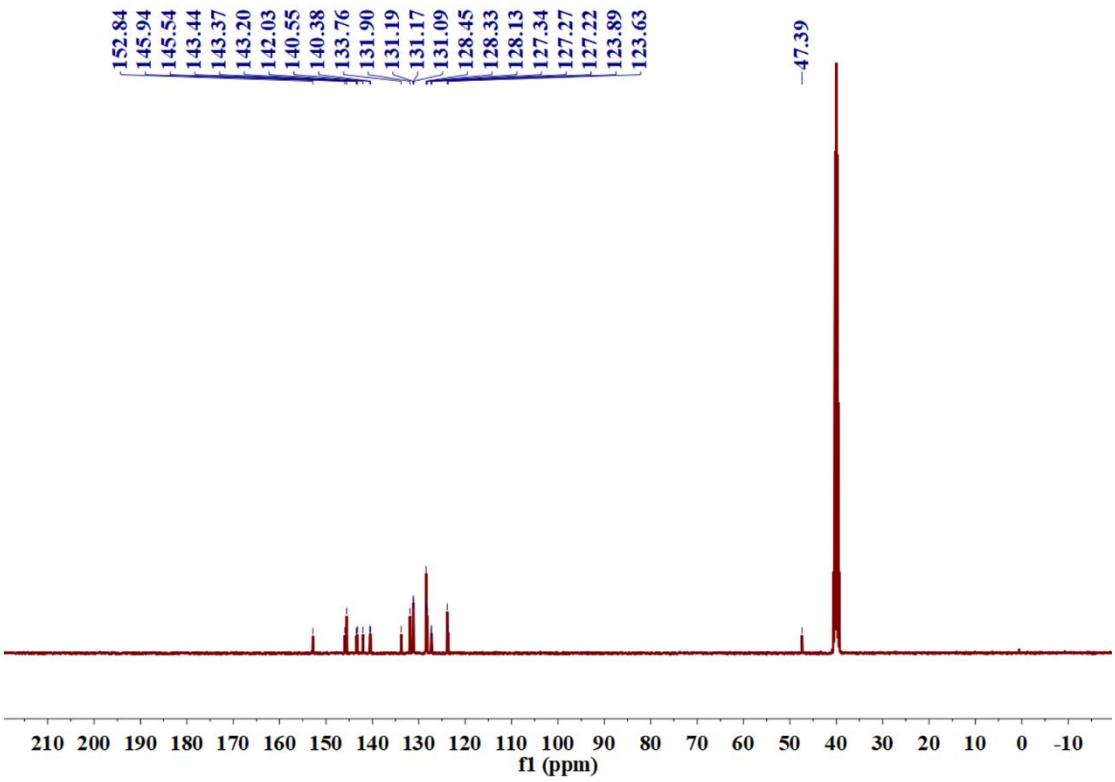

Supplementary Figure 3. ^{13}C NMR spectra of **TPE-Py-I** in DMSO-d_6.

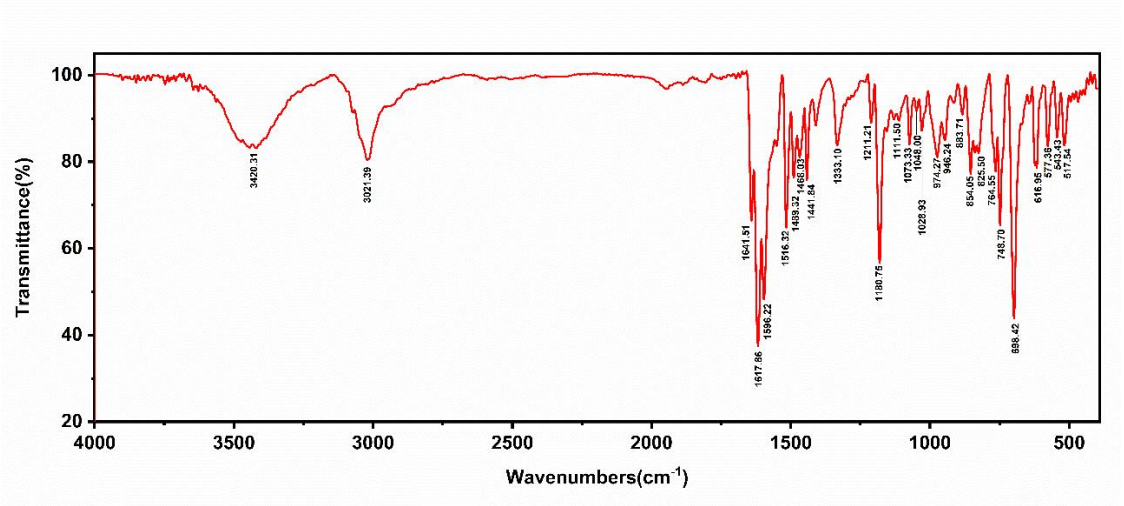

Supplementary Figure 4. Infrared spectroscopy (IR) of **TPE-Py-I**.

9. ^{1}H NMR titration experiment

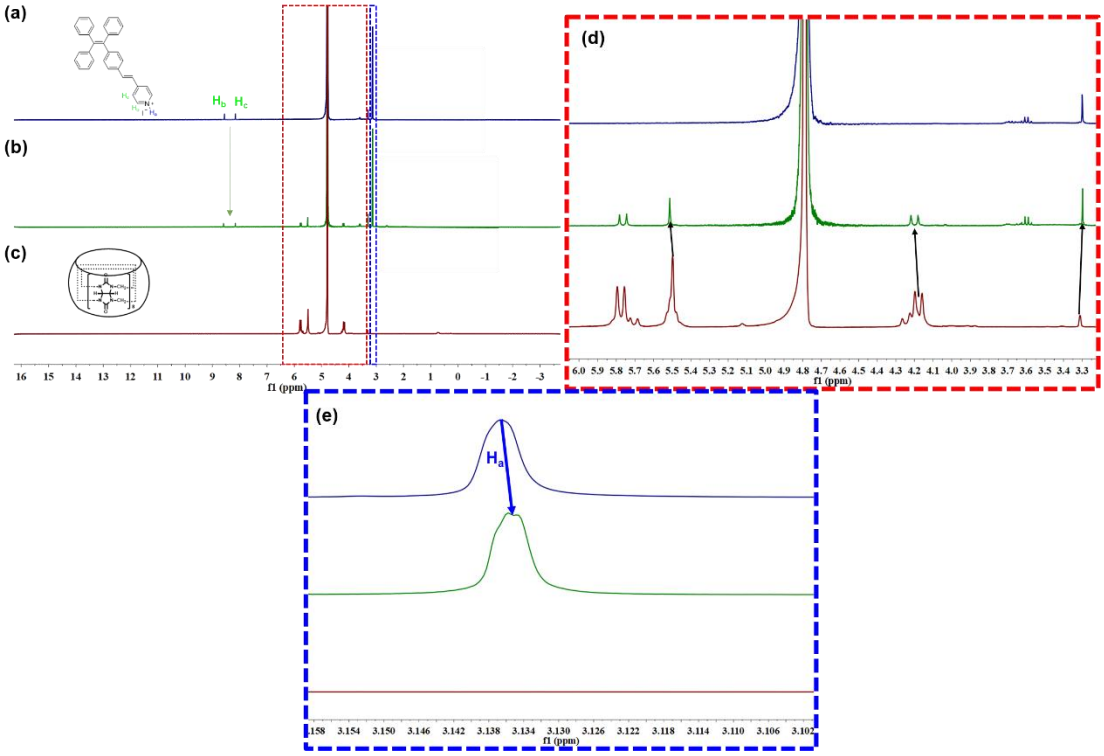

Supplementary Figure 5. (A) ^{1}H NMR spectrum of **TPE-Py-I** in D_2O; (B) ^{1}H NMR spectrum of **2TPE-Py-I@CB[8]** in D_2O; (C) ^{1}H NMR spectrum of **CB[8]** in D_2O; (D) Enlarged view of ^{1}H NMR spectrum of the **CB[8]** section; (E) Enlarged view of ^{1}H NMR spectrum of the H_a section. [TPE-Py-I=1.0 mM, CB[8]=0.5 mM]

Supplementary Table 1. ^{1}H-NMR chemical shift ( ) of CB[8], TPE-Py-I and 2TPE-Py-I@CB[8] inclusion complex, and their complexation induced shift (CIS, $\delta_{complex} - \delta$).

^{1}H Proton NMR [Chemical Shifts (δ), ppm]				
	CB[8]	TPE-Py-I	2TPE-Py-I@CB[8]	CIS (Δδ)
H_a	--	3.1381	3.1358	-0.0023
H_b	--	8.8439	8.8439	0
H_c	--	8.1728	8.1728	0
	5.7946	--	5.7828	-0.0118
	5.4976	--	5.5131	0.0155
	4.1974	--	4.2188	0.0214
	3.3135	--	3.2984	-0.0151

10. UV-vis absorption and fluorescence emission spectra

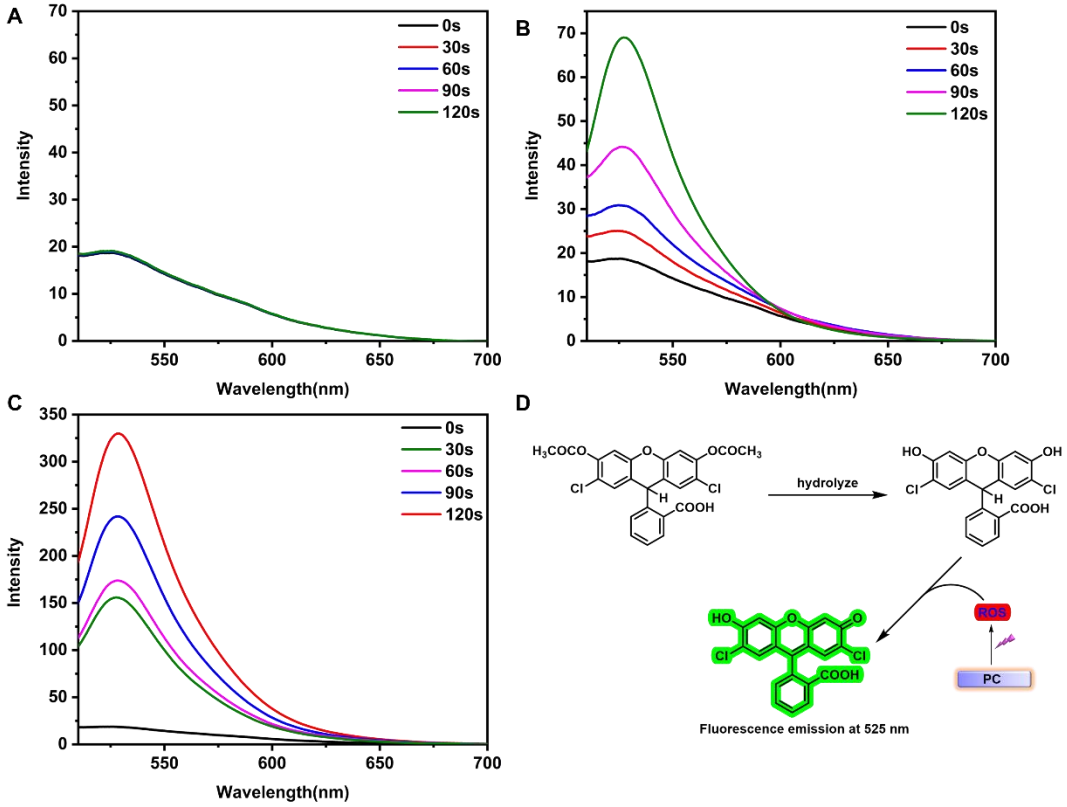

Supplementary Figure 6. Fluorescence emission spectra of DCFH-DA upon purple light irradiation from 0 to 120 s in the presence of the (A) 20 μM DCFH-DA in H_2O, (B) 20 μM TPE-Py-I + 20 μM DCFH-DA in H_2O, (C) and 20 μM 2TPE-Py-I@CB[8] + 20 μM DCFH-DA in H_2O; (D) The mechanism of DCFH-DA as the ROS scavenger for monitoring ROS in the aqueous solution.

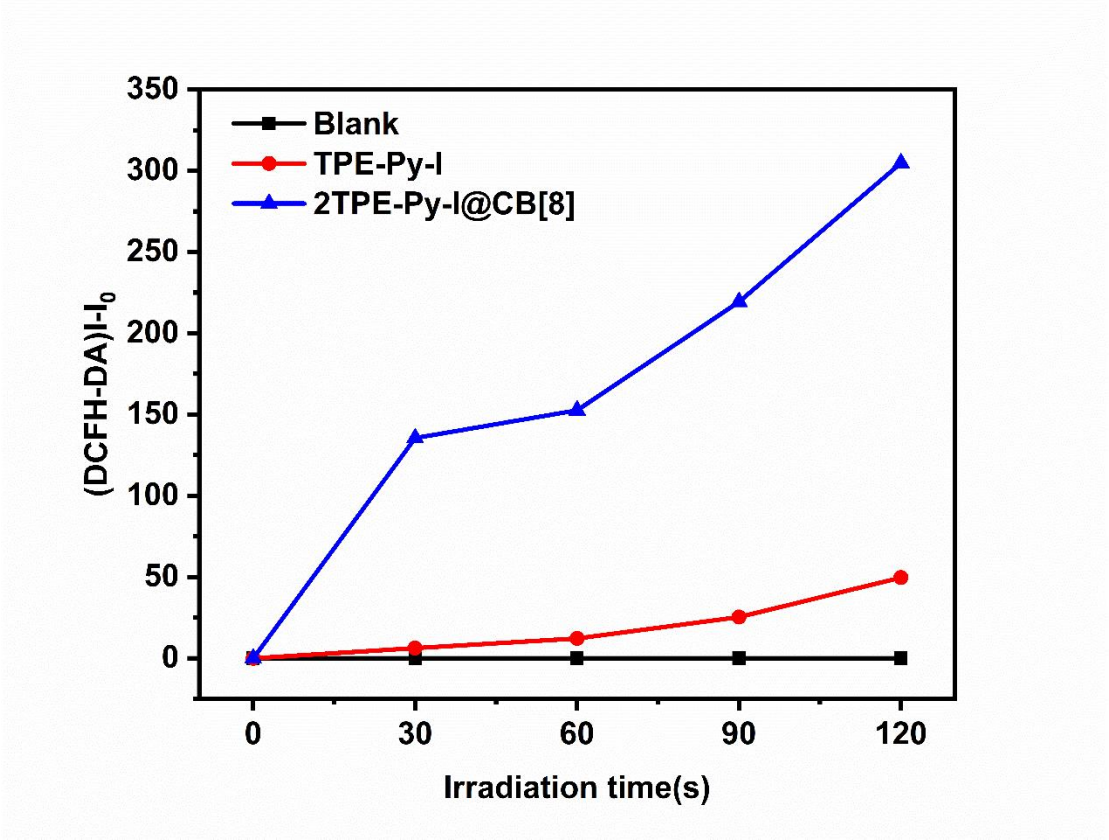

Supplementary Figure 7. Plots of ΔIntensity($I–I_0$) for DCFH-DA at 525 nm (λ_{ex}=485 nm) upon purple light irradiated for different times in the presence of DCFH-DA, TPE-Py-I+DCFH-DA or 2TPE-Py-I @CB[8]+ DCFH-DA.

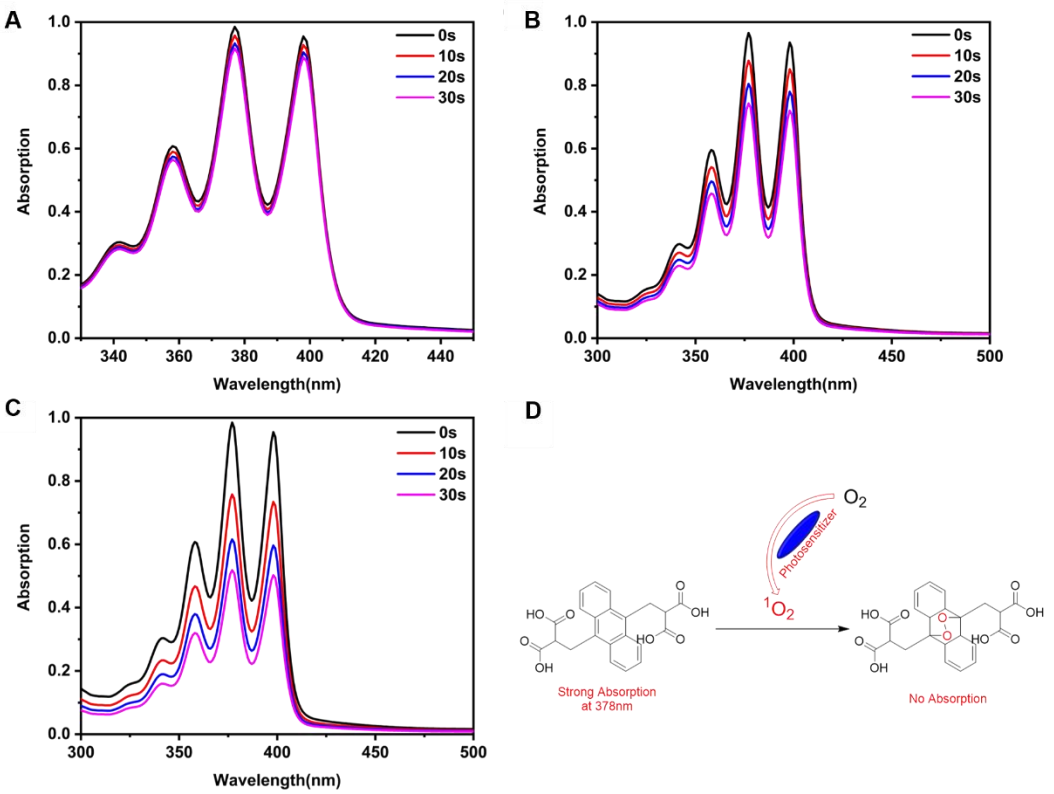

Supplementary Figure 8. UV-vis spectra of ABDA upon purple LED irradiation from 0 to 30 s in the presence of the (A) and 50 μM ABDA in H_2O, (B) 20 μM TPE-Py-I + 50 μM ABDA in H_2O, (C) 20 μM 2TPE-Py-I@CB[8] + 50 μM ABDA in H_2O; (D) The mechanism of 9,10-anthracenediyl-bis(methylene)-dimalonic acid (ABDA) as the $^1O_2$ scavenger for monitoring $^1O_2$ generation in the solution.

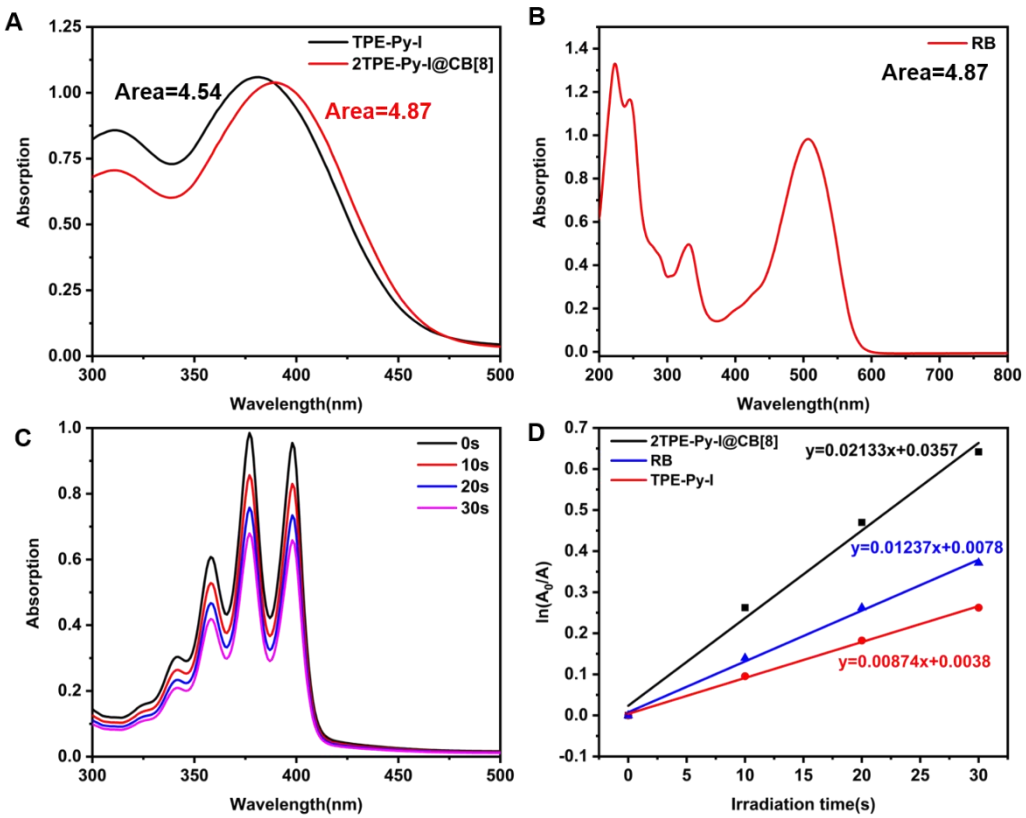

Supplementary Figure 9. (A) UV-vis absorption spectrum and integration area of TPE-Py-I and 2TPE-Py-I@CB[8]; (B) UV-vis absorption spectrum and integration area of RB; (C) UV-vis spectra of ABDA upon purple LED irradiation from 0 to 30 s in the presence of the 20 μM RB + 50 μM ABDA in H_2O; (D) Plot of the absorbance at 378 nm of ABDA against exposure time in the presence of RB, TPE-Py-I, and 2TPE-Py-I@CB[8].

11. ^{1}H NMR and ^{13}C NMR spectra and data of 2a-2o

2a. triphenylphosphine oxide[4]

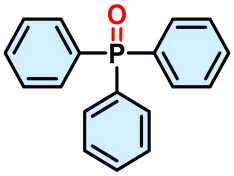

White solid (50.0 mg); 90% yield; eluent: PE/EA = 1:1; ^{1}H NMR (400 MHz, $CDCl_3$) δ 7.67 (dd, J = 12.0, 7.4 Hz, 6H), 7.54 (d, J = 7.3 Hz, 3H), 7.47 (d, J = 7.7 Hz, 6H). ^{13}C NMR (101 MHz, $CDCl_3$) δ 133.0, 132.0 (d, J = 9.8 Hz), 131.9 (d, J = 2.8 Hz), 128.4 (d, J = 12.1 Hz). m.p.: 157-159℃

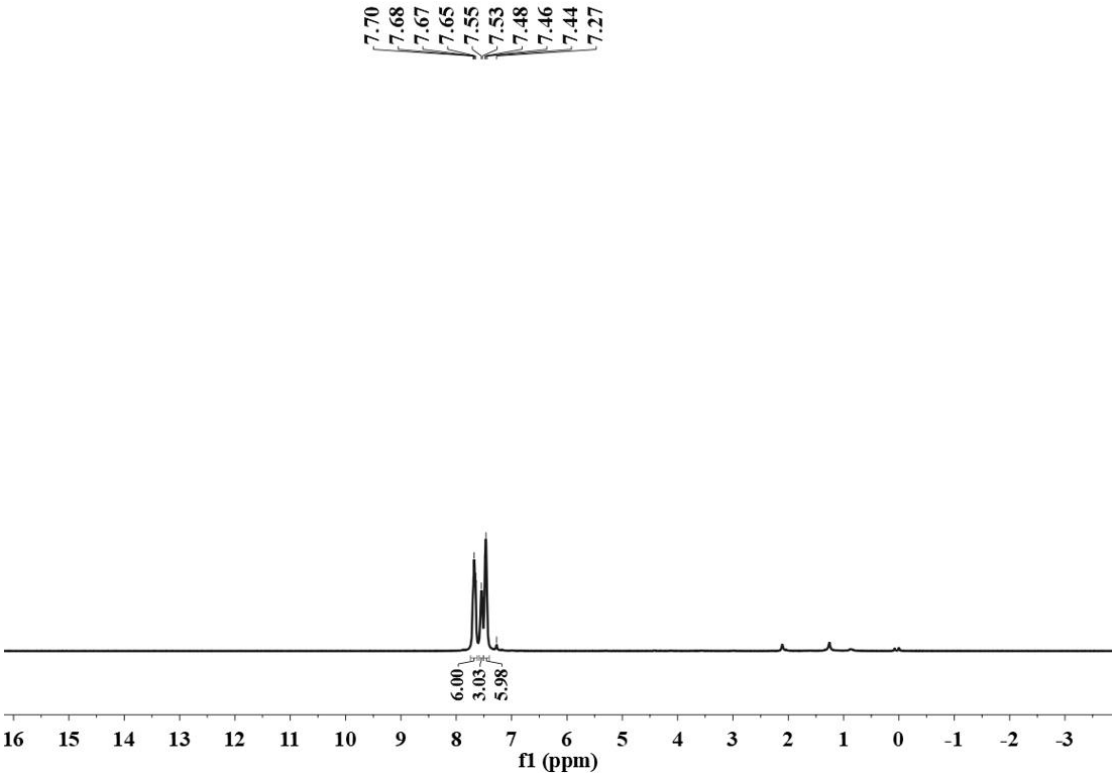

Supplementary Figure 10. ^{1}H NMR spectra of **2a** in $CDCl_3$.

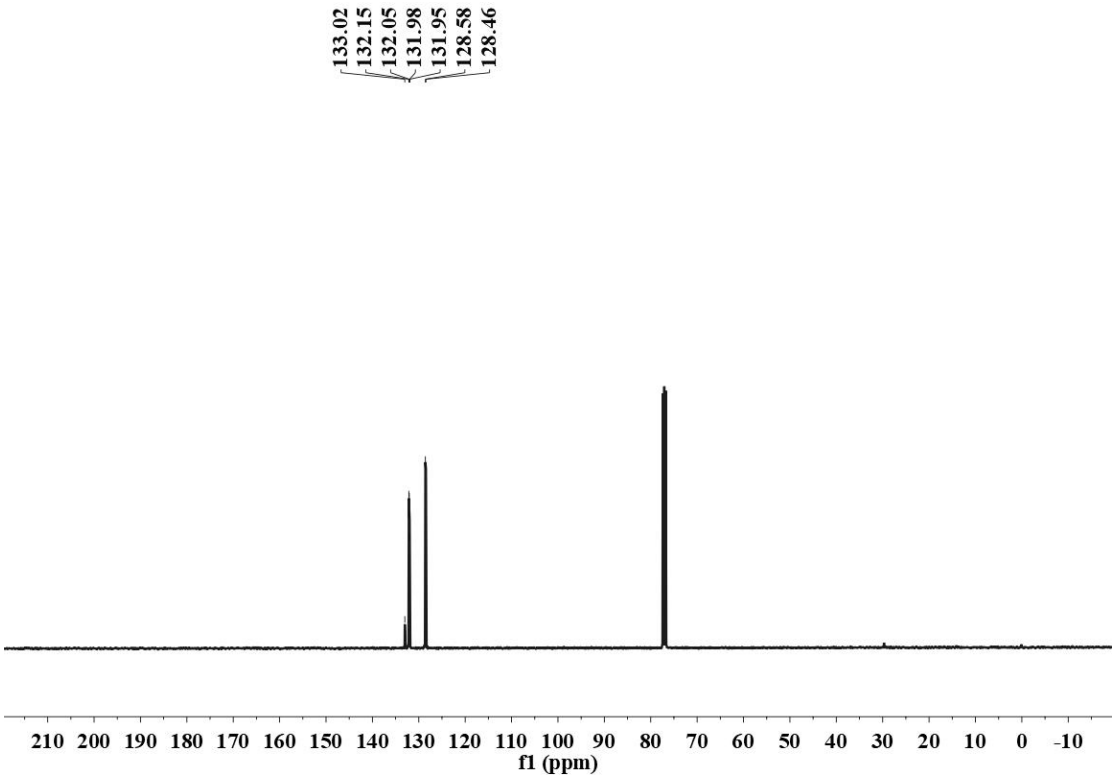

Supplementary Figure 11. ^{13}C NMR spectra of **2a** in $CDCl_3$.

2b. tris(4-fluorophenyl)phosphine oxide[5]

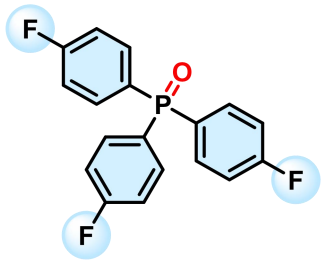

White solid (59.0 mg); 89% yield; eluent: PE/EA = 1:1; ^{1}H NMR (400 MHz, $CDCl_3$) δ 7.57 (m, 6H), 7.10 (m, 6H). ^{13}C NMR (101 MHz, $CDCl_3$) δ 165.2 (dd, J = 254.3, 3.0 Hz), 134.5 (dd, J = 11.4, 8.8 Hz), 128.1 (d, J = 108.1 Hz), 116.2 (dd, J = 21.5, 13.3 Hz). m.p.: 157-159°C

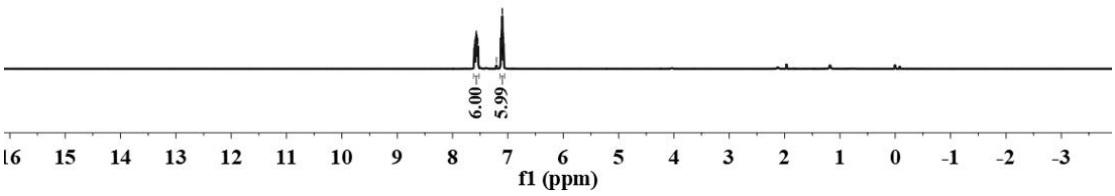

Supplementary Figure 12. ^{1}H NMR spectra of **2b** in $CDCl_3$.

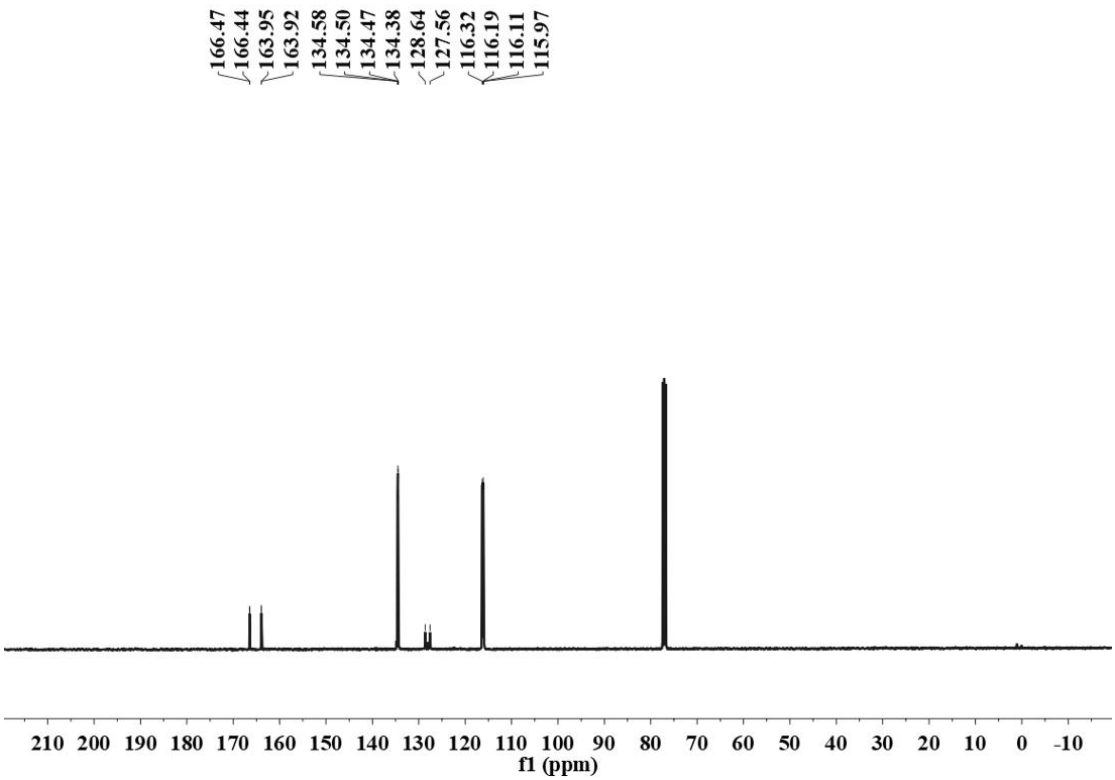

Supplementary Figure 13. ^{13}C NMR spectra of **2b** in $CDCl_3$.

2c. tris(4-chlorophenyl)phosphine oxide[4]

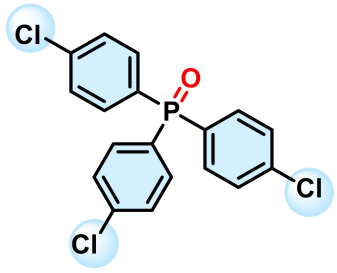

White solid (70.0 mg); 92% yield; eluent: PE/EA = 1:1; ^{1}H NMR (400 MHz, $CDCl_3$) δ 7.60 - 7.52 (m, 6H), 7.45 (m, 6H). ^{13}C NMR (101 MHz, $CDCl_3$) δ 139.10 (d, J = 3.4 Hz), 133.28 (d, J = 10.9 Hz), 130.23 (d, J = 106.6 Hz), 129.11 (d, J = 12.8 Hz). m.p.: 172-174℃.

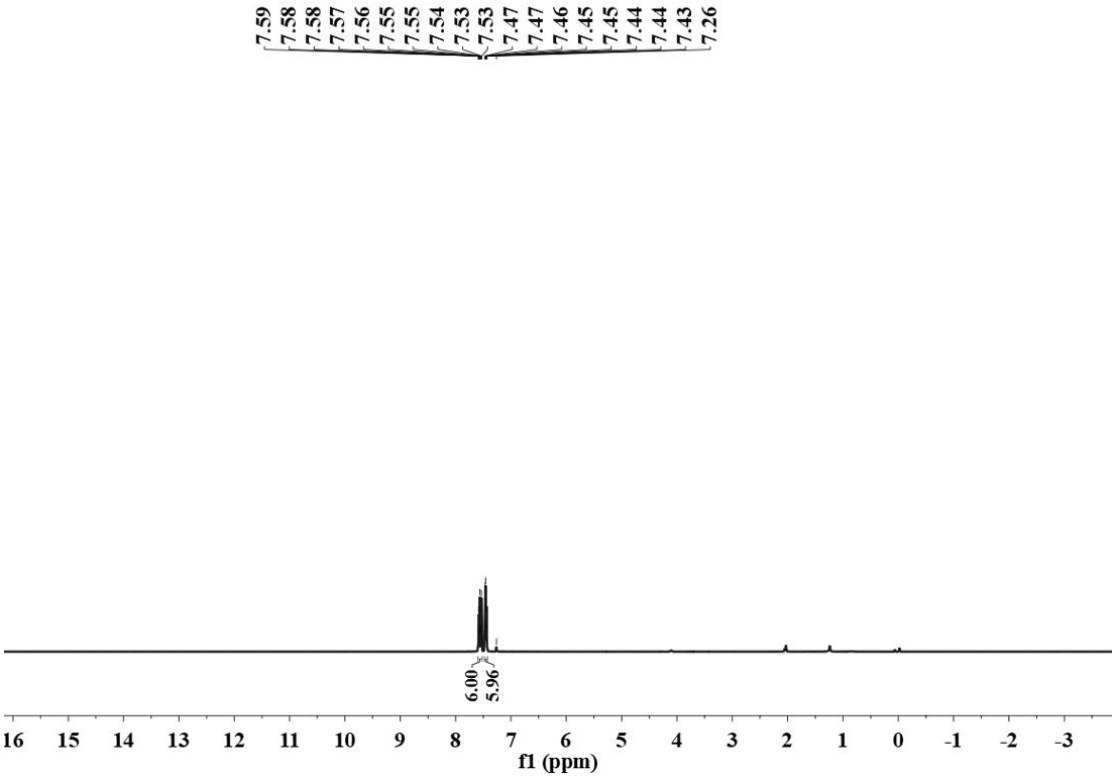

Supplementary Figure 14. ^{1}H NMR spectra of **2c** in $CDCl_3$.

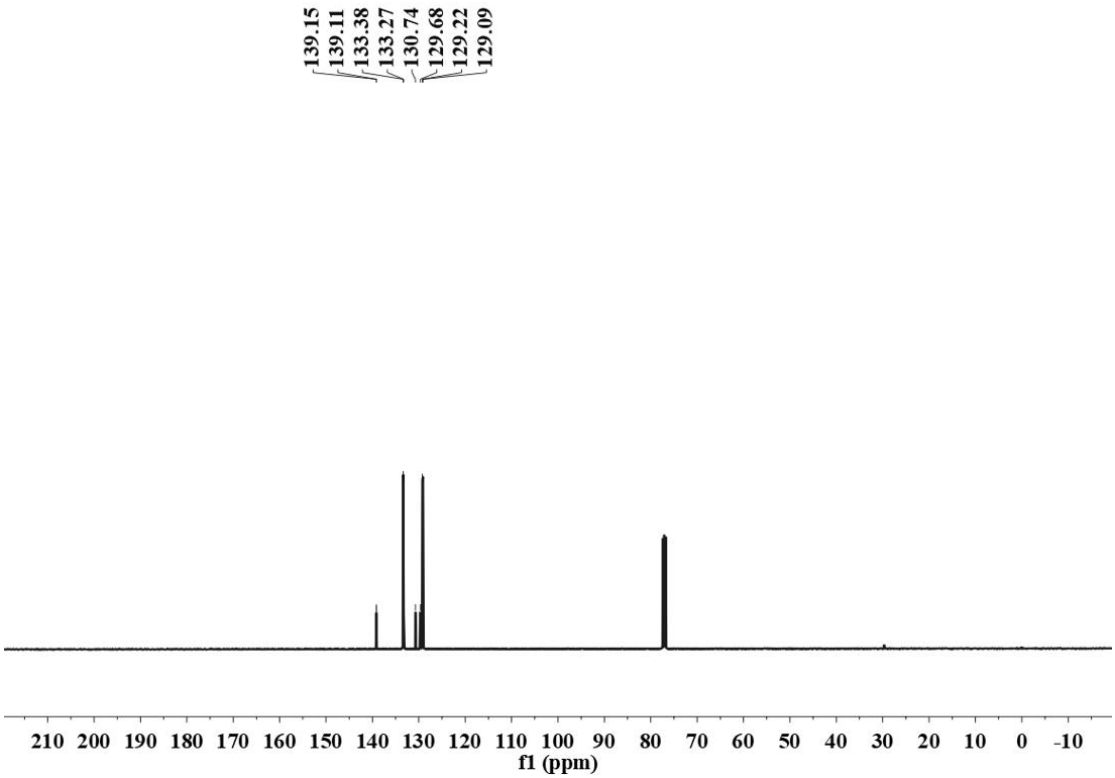

Supplementary Figure 15. ^{13}C NMR spectra of **2c** in $CDCl_3$.

2d. tri-*p*-tolylphosphine oxide[5]

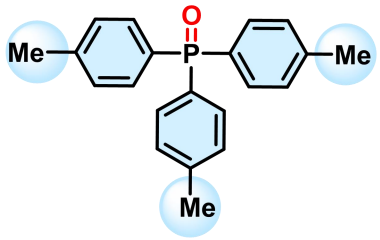

White solid (52.5 mg); 82% yield; eluent: PE/EA = 1:1; ^{1}H NMR (400 MHz, $CDCl_3$) δ 7.59 - 7.49 (m, 6H), 7.25 (dd, J = 8.1, 2.6 Hz, 6H), 2.39 (s, 9H). ^{13}C NMR (101 MHz, $CDCl_3$) δ 142.2 (d, J=3.0 Hz), 132.1 (d, J=10.1 Hz), 130.2, 129.2 (d, J=13.1 Hz), 21.6. m.p.: 135 - 137℃

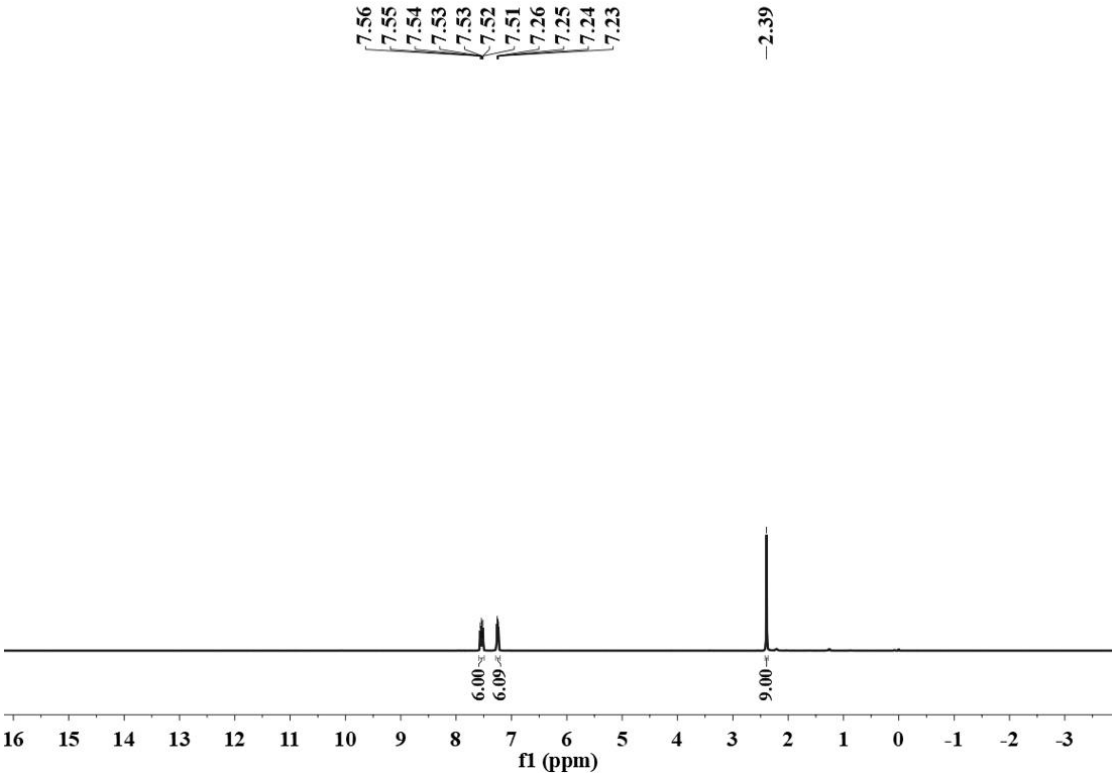

Supplementary Figure 16. ^{1}H NMR spectra of **2d** in $CDCl_3$.

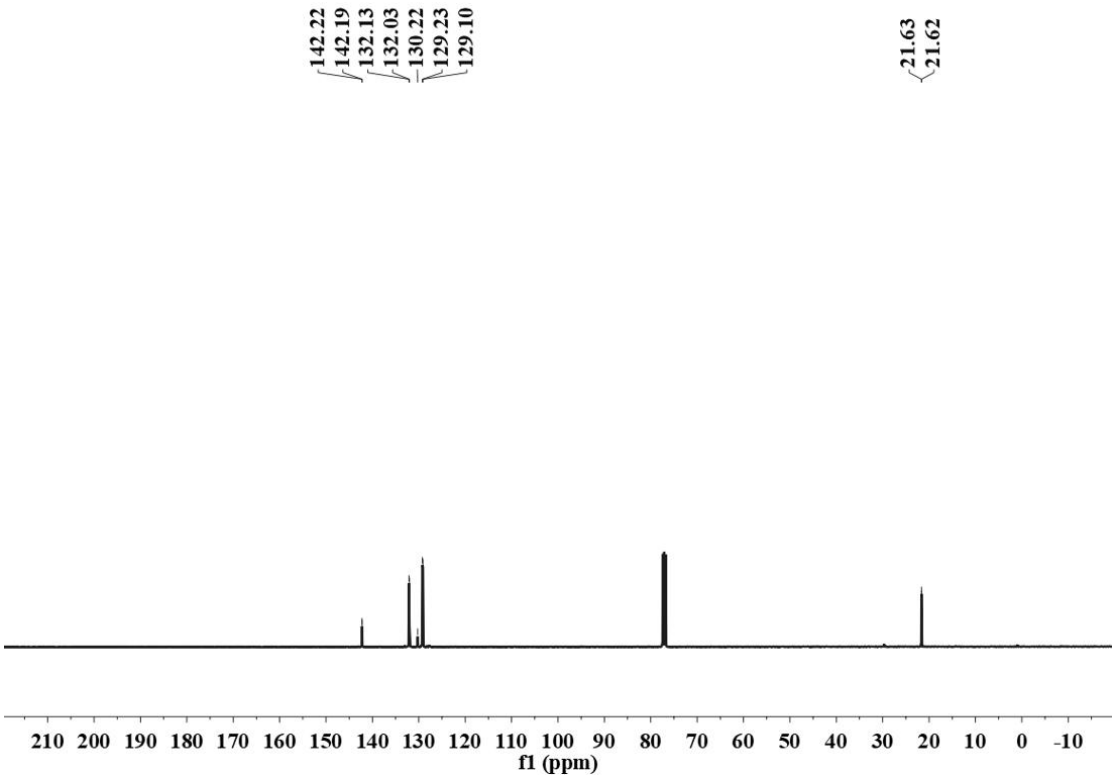

Supplementary Figure 17. ^{13}C NMR spectra of **2d** in $CDCl_3$.

2e. tris(3-fluorophenyl)phosphine oxide[4]

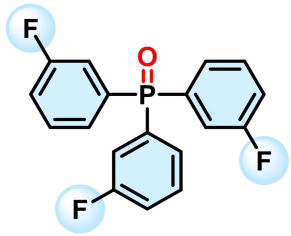

White solid (55.7 mg); 84% yield; eluent: PE/EA = 1:1; ^{1}H NMR (400 MHz, $CDCl_3$) δ 7.30 (m, 6H), 7.23 - 7.06 (m, 6H). ^{13}C NMR (101 MHz, $CDCl_3$) δ 162.6 (dd, J = 251.2, 17.2 Hz), 134.5 (d, J = 5.7 Hz), 133.5 (d, J = 5.6 Hz), 130.9 (dd, J = 14.3, 7.4 Hz), 127.7 (dd, J = 9.5, 3.3 Hz), 119.8 (dd, J = 21.0, 2.5 Hz), 118.9 (dd, J = 22.5, 10.9 Hz). m.p.: 105-107℃.

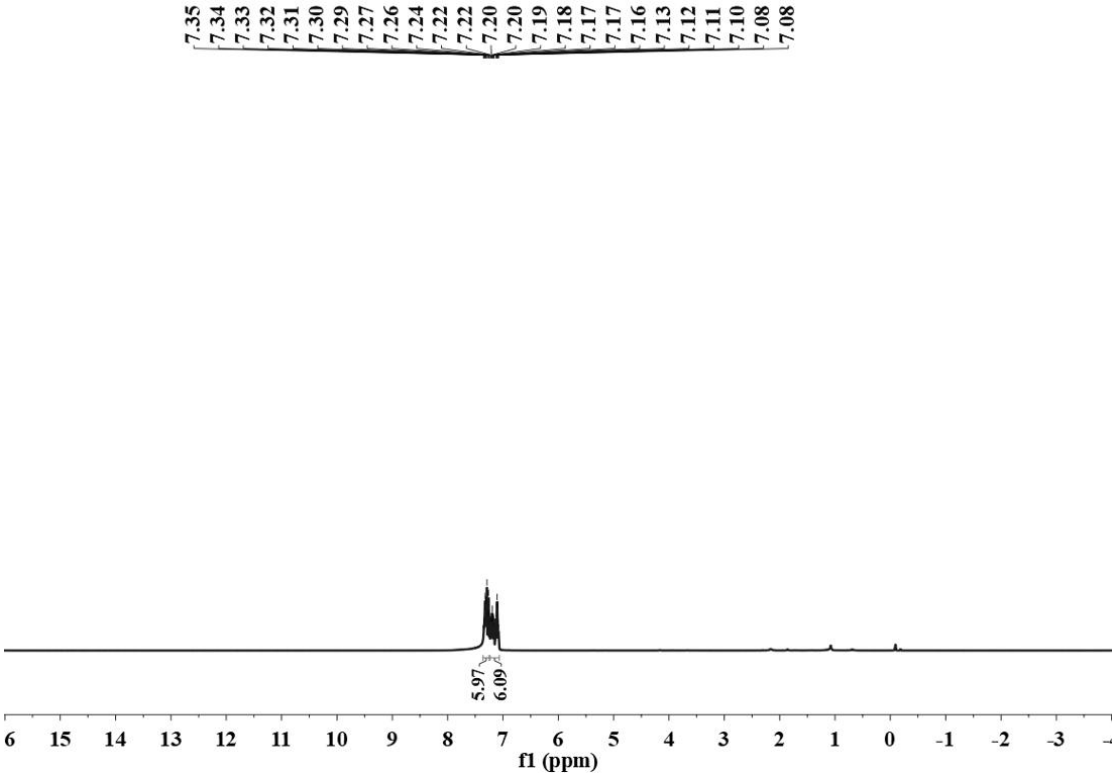

Supplementary Figure 18. ^{1}H NMR spectra of **2e** in $CDCl_3$.

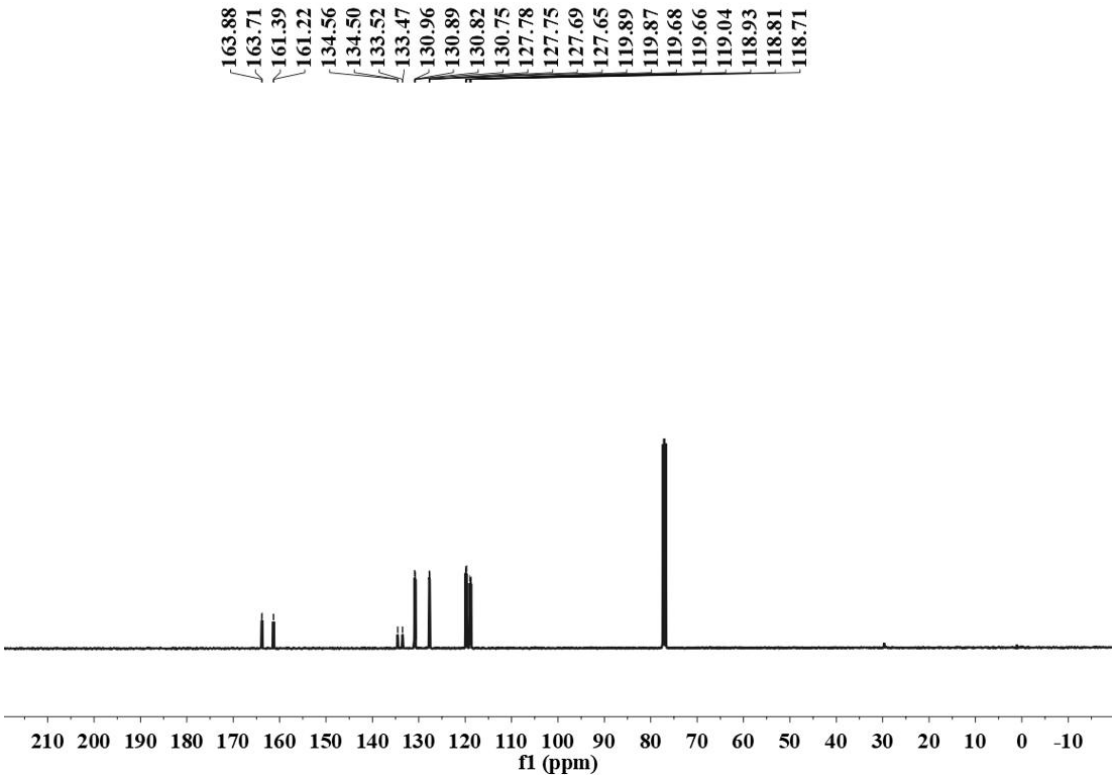

Supplementary Figure 19. ^{13}C NMR spectra of **2e** in $CDCl_3$.

2f. tri-*m*-tolylphosphine oxide[5]

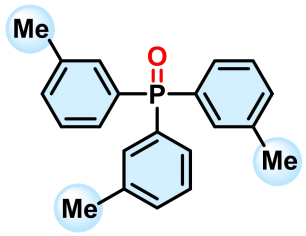

White solid (47.9 mg); 75% yield; eluent: PE/EA = 1:1; ^{1}H NMR (400 MHz, $CDCl_3$) δ 7.58 (d, J = 12.4 Hz, 3H), 7.42 - 7.30 (m, 9H), 2.36 (s, 9H). ^{13}C NMR (101 MHz, $CDCl_3$) δ 138.4 (d, J = 12.1 Hz), 133.01, 132.6 (d, J = 3.0 Hz), 132.5 (d, J = 9.1 Hz) , 131.9, 129.2 (d, J = 10.1 Hz), 128.3 (d, J = 13.1 Hz), 21.47. m.p.: 112 - 113℃.

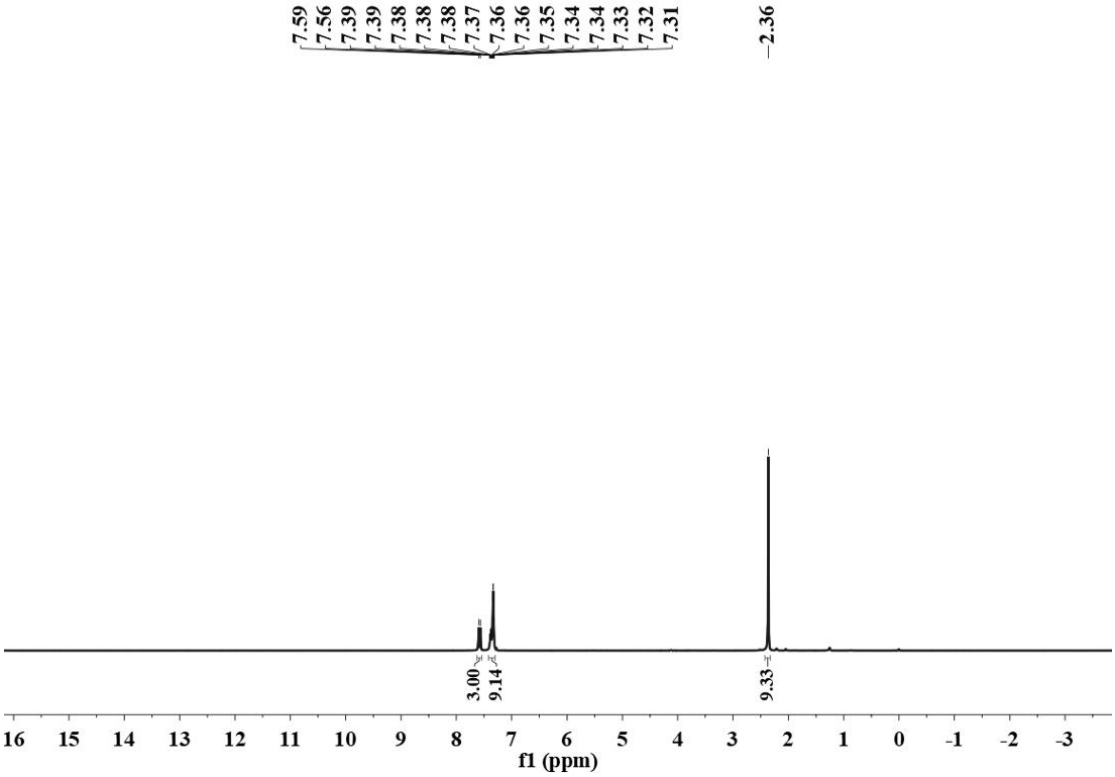

Supplementary Figure 20. ^{1}H NMR spectra of **2f** in $CDCl_3$.

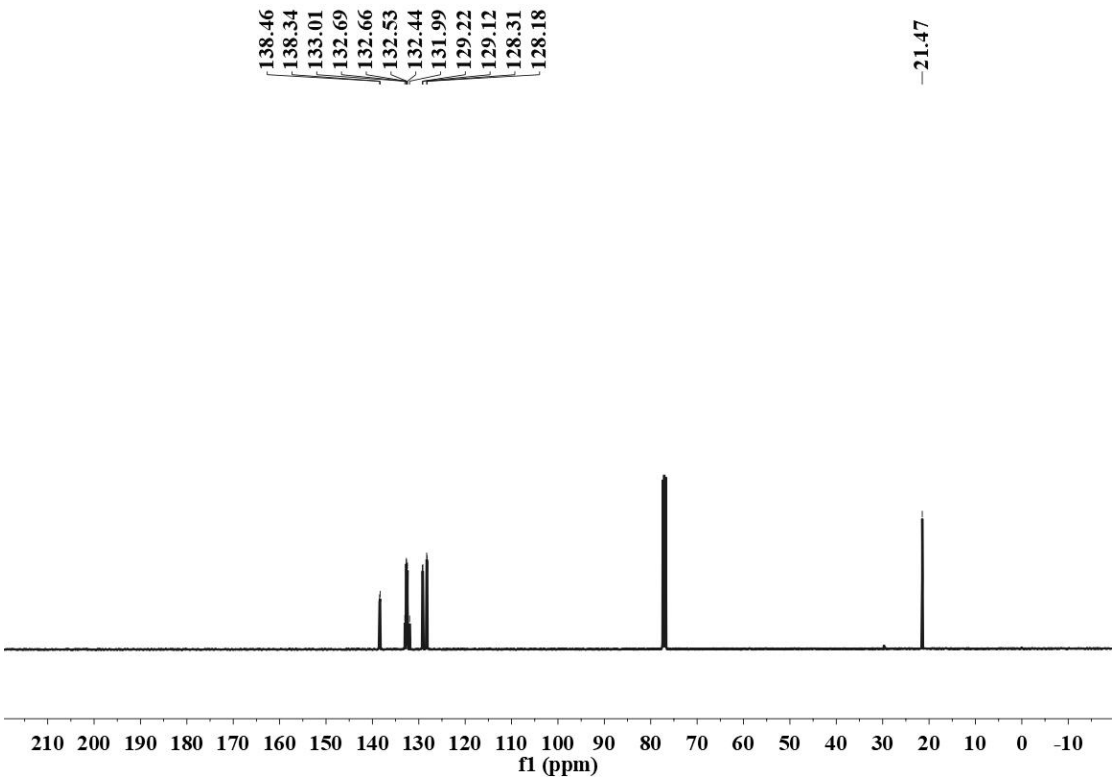

Supplementary Figure 21. ^{13}C NMR spectra of **2f** in $CDCl_3$.

2g. tris(3-methoxyphenyl)phosphine oxide[4]

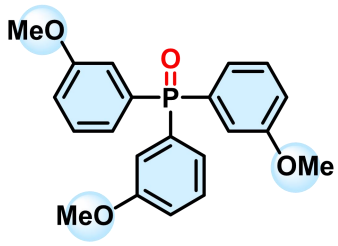

White solid (52.9 mg); 72% yield; eluent: PE/EA = 1:1; ^{1}H NMR (400 MHz, $CDCl_3$) δ 7.39 - 7.24 (m, 6H), 7.20 - 7.00 (m, 6H), 3.87 - 3.70 (m, 9H). ^{13}C NMR (101 MHz, $CDCl_3$) δ 159.6 (d, J = 15.1 Hz), 134.2, 133.1, 129.7 (d, J = 13.4 Hz), 124.4 (d, J = 10.1 Hz), 118.3 (d, J = 3.0 Hz), 116.7 (d, J = 9.1 Hz), 55.5. m.p.: 152-154℃.

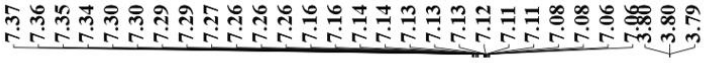

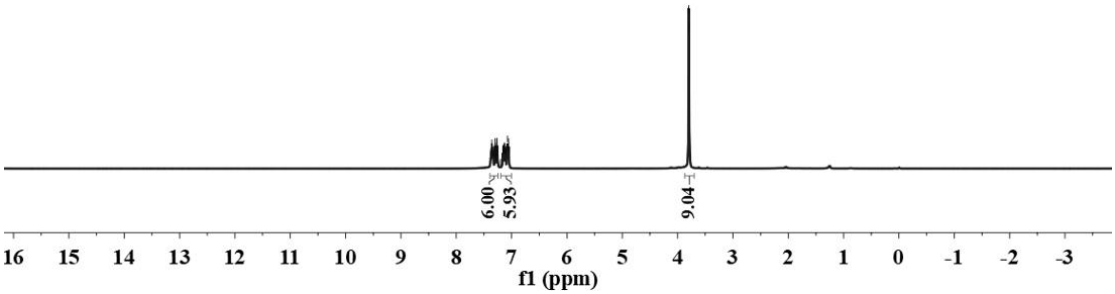

Supplementary Figure 22. ^{1}H NMR spectra of **2g** in $CDCl_3$.

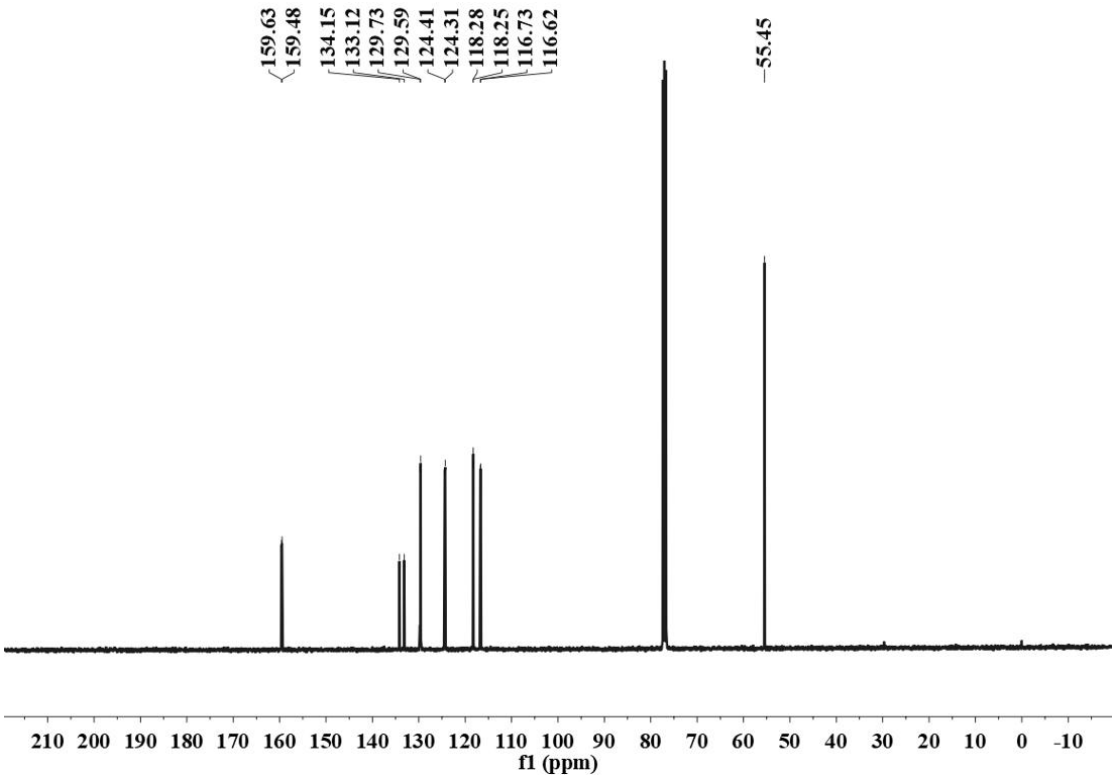

Supplementary Figure 23. ^{13}C NMR spectra of **2g** in $CDCl_3$.

2h. diphenyl(pyridin-2-yl)phosphine oxide[4]

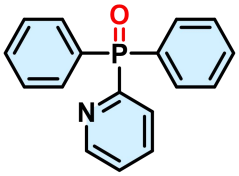

White solid (51.5 mg); 91% yield; eluent: PE/EA = 1:1; ^{1}H NMR (400 MHz, $CDCl_3$) δ 8.80 - 8.75 (m, 1H), 8.31 (t, J = 6.7 Hz, 1H), 7.92 - 7.86 (m, 4H), 7.84 (m, 1H), 7.51 (m, 2H), 7.44 (m, 4H), 7.38 (s, 1H). ^{13}C NMR (101 MHz, $CDCl_3$) δ 157.1, 155.7, 150.3 (d, J = 19.1 Hz), 136.3 (d, J = 9.1 Hz), 132.7, 132.2 (d, J =10.1 Hz), 132.0 (d, J = 3.0. Hz), 131.7, 128.6 (d, J = 5.0 Hz), 128.4 (d, J = 18.1 Hz), 125.4 (d, J = 3.0 Hz), 124.1. m.p.: 108-110℃.

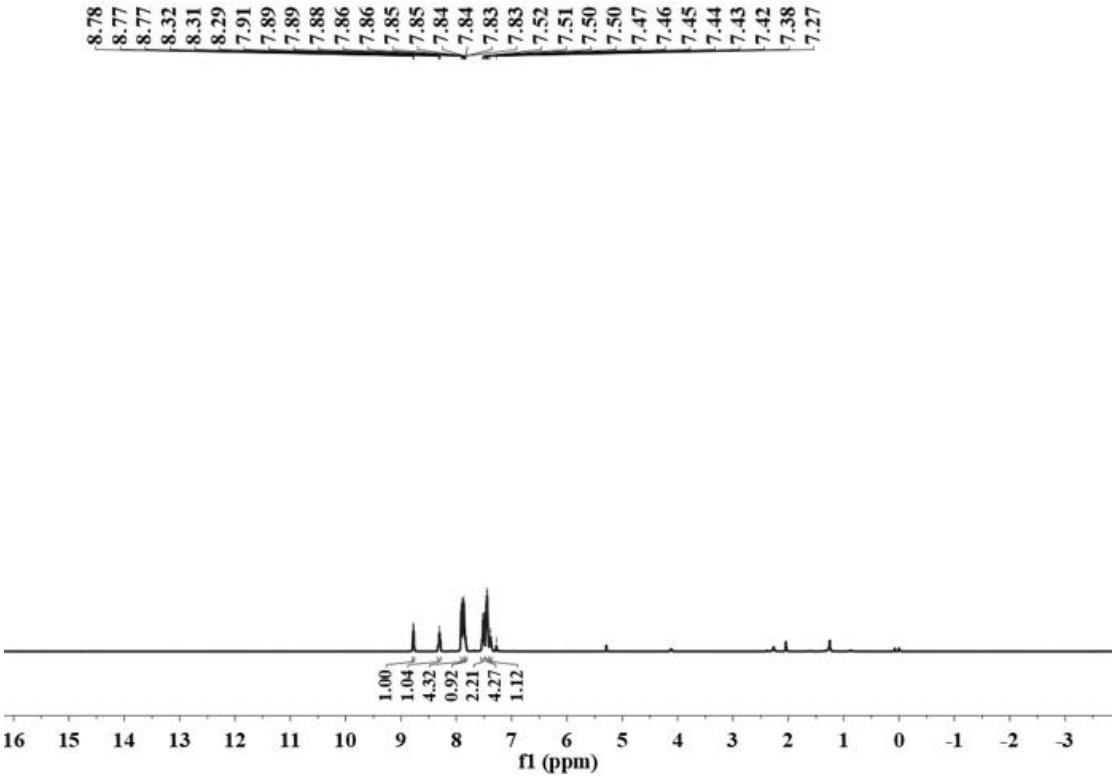

Supplementary Figure 24. ^{1}H NMR spectra of **2h** in $CDCl_3$.

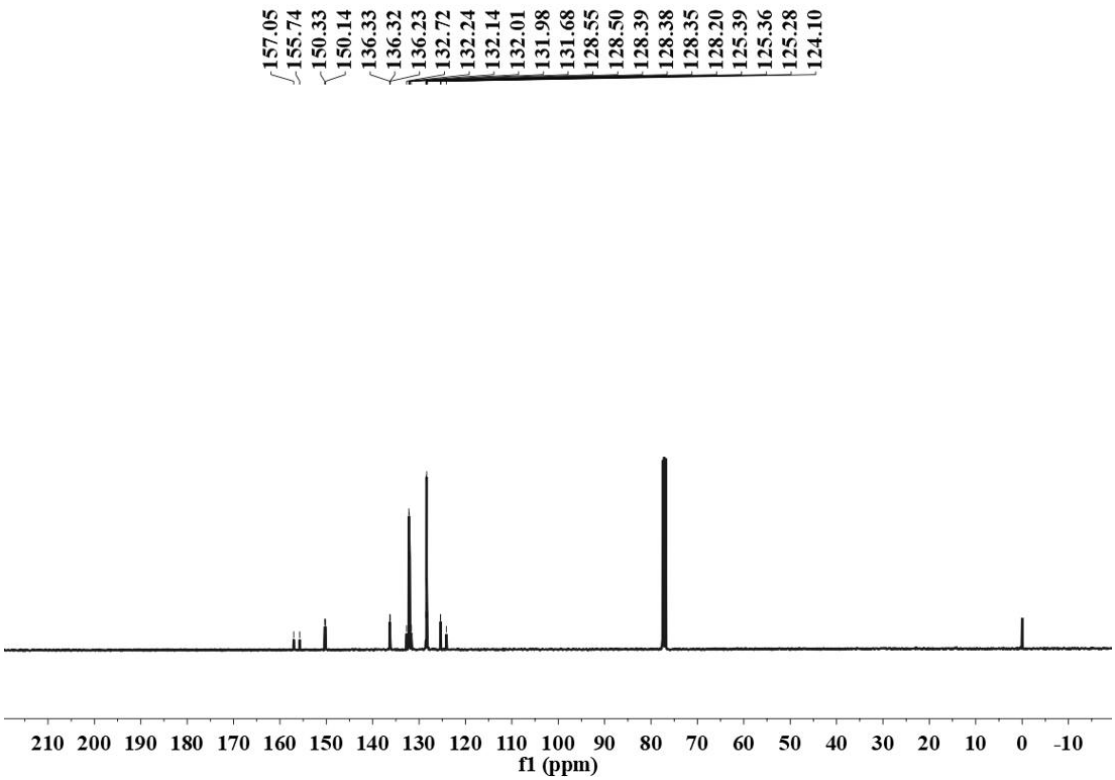

Supplementary Figure 25. ^{13}C NMR spectra of **2h** in $CDCl_3$.

2i. [1,1'-biphenyl]-3-yldiphenylphosphine oxide[6]

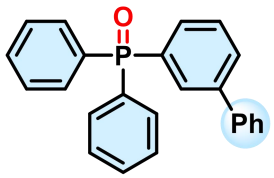

White solid (62.3 mg); 88% yield; eluent: PE/EA = 1:1; ^{1}H NMR (400 MHz, $CDCl_3$) δ 7.57 (dd, J = 11.2, 7.9 Hz, 5H), 7.44 - 7.26 (m, 9H), 7.04 (dd, J = 7.3, 2.3 Hz, 3H). ^{13}C NMR (101 MHz, $CDCl_3$) δ 147.7 (d, J = 9.1 Hz), 140.3 (d, J = 5.0 Hz), 134.1 (d, J = 12.1 Hz), 133.6, 132.5, 132.2, 132.0 (d, J = 15.1 Hz), 131.7(d, J = 2.0 Hz), 131.6 (d, J = 10.1 Hz), 131.2 (d, J = 3.0 Hz), 130.2, 128.2 (d, J = 12.1 Hz), 127.2 (d, J = 7.0 Hz), 126.6 (d, J = 13.1 Hz). m.p.: 150 - 154 °C.

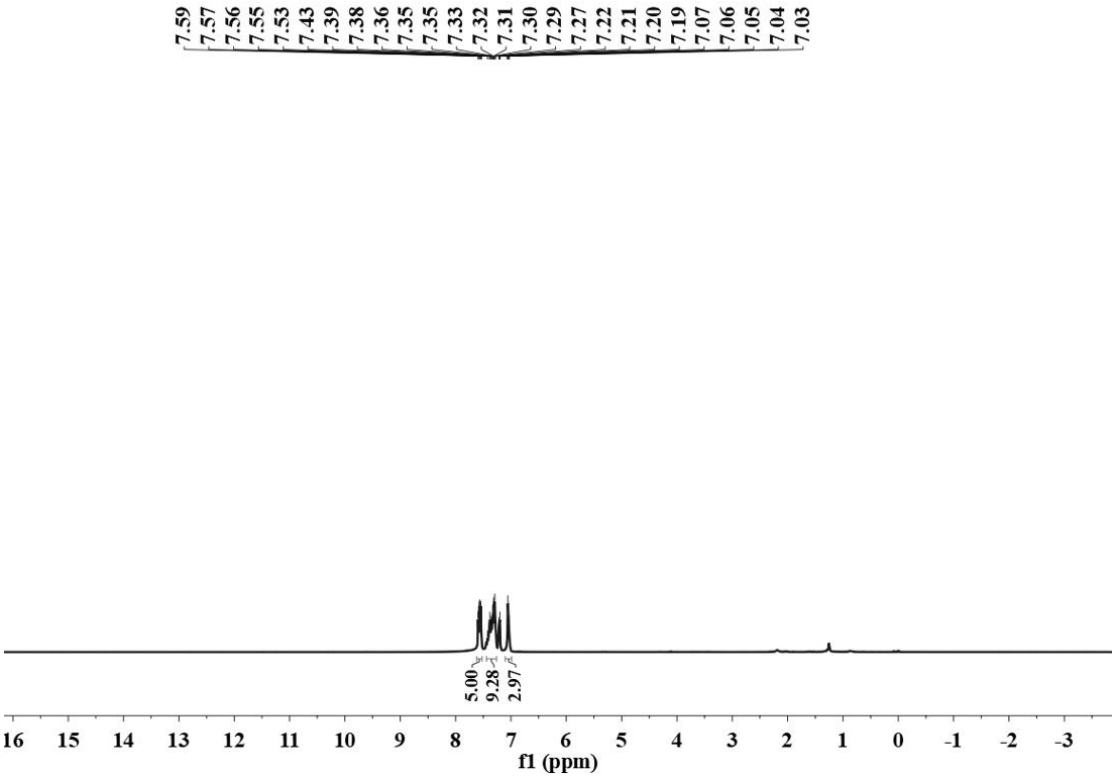

Supplementary Figure 26. ^{1}H NMR spectra of **2i** in $CDCl_3$.

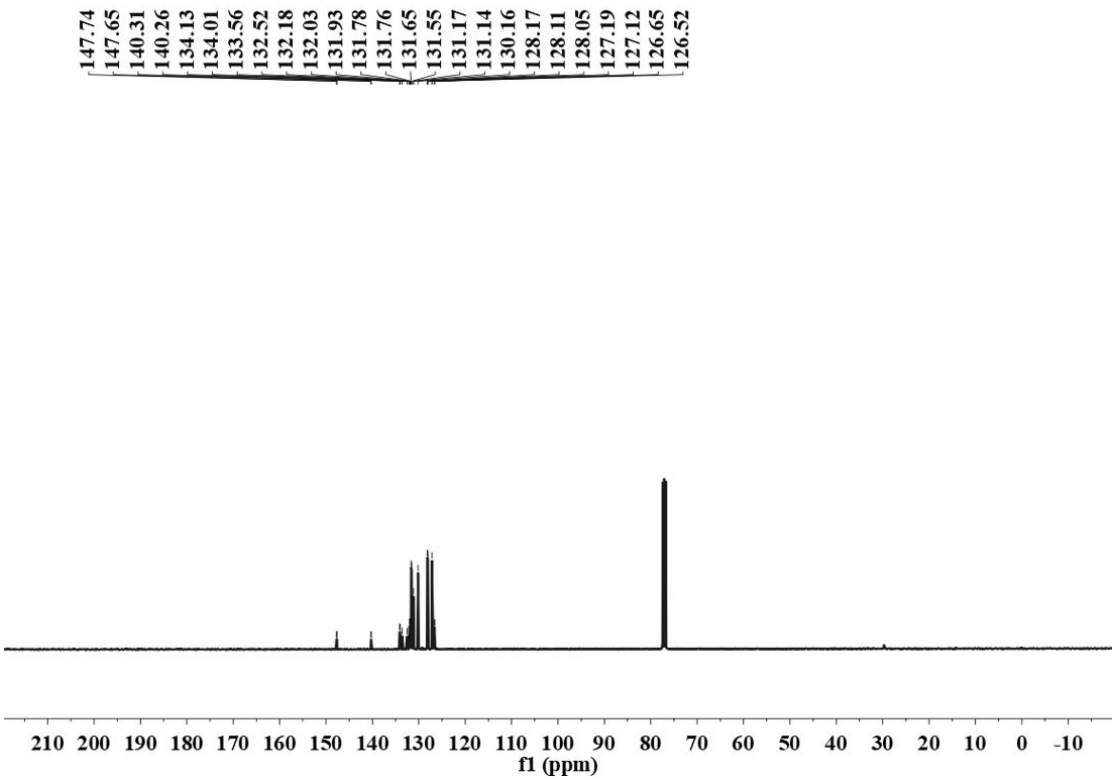

Supplementary Figure 27. ^{13}C NMR spectra of **2i** in $CDCl_3$.

2j. 3-(diphenylphosphoryl)benzoic acid[4]

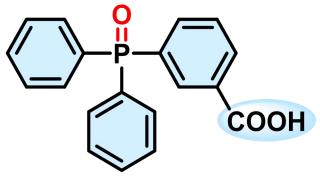

White solid (52.1 mg); 81% yield; PE/MeOH = 1:1; ^{1}H NMR (400 MHz, $CDCl_3$) δ 7.96 (s, 1H), 7.40 (s, 6H), 7.16 (d, J = 7.6 Hz, 6H), 6.95 - 6.85 (m, 1H), 3.88 (s, 1H). ^{13}C NMR (101 MHz, $CDCl_3$) δ 172.1, 143.5, 134.8, 134.1, 133.5 (d, J = 10.1 Hz), 132.0, 131.5, 130.9, 129.6, 128.1 (d, J = 10.1 Hz). m.p.: 272-274℃.

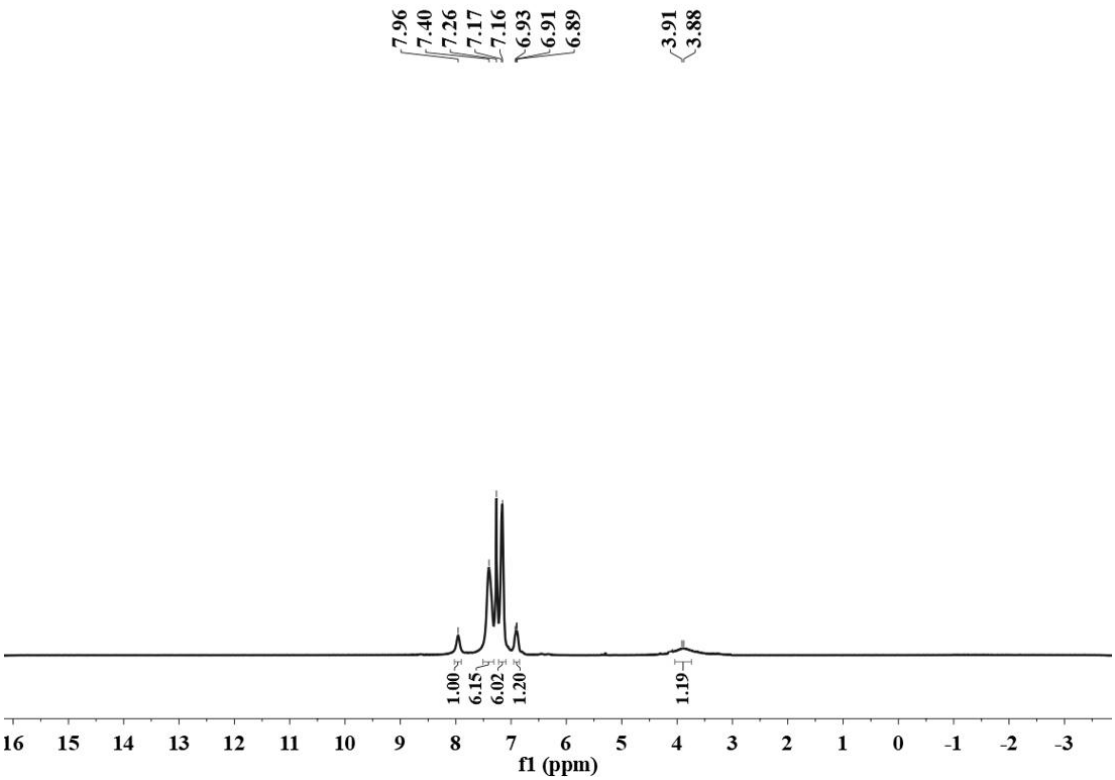

Supplementary Figure 28. ^{1}H NMR spectra of **2j** in $CDCl_3$.

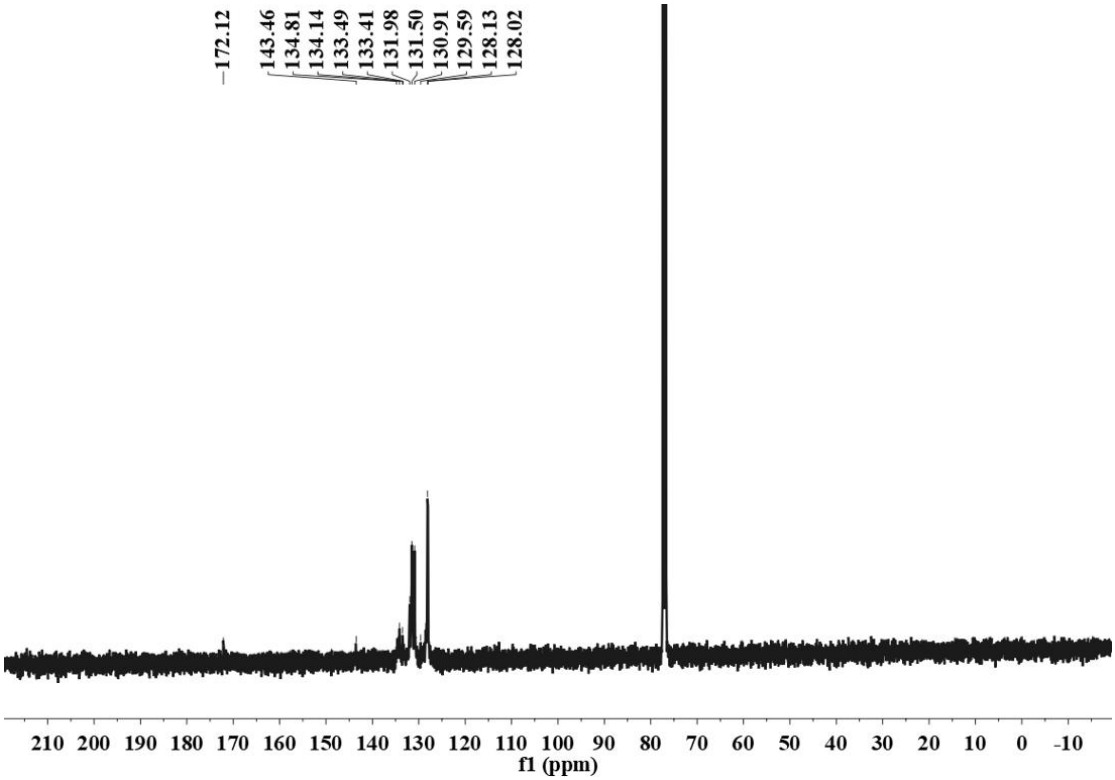

Supplementary Figure 29. ^{13}C NMR spectra of **2j** in $CDCl_3$.

2k. diphenyl(propyl)phosphine oxide [7]

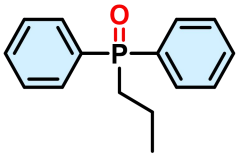

White solid (42.5 mg); 87% yield; eluent: PE/EA = 1:1; ^{1}H NMR (400 MHz, $CDCl_3$) δ 7.78 - 7.70 (m, 4H), 7.54 - 7.43 (m, 6H), 2.30 - 2.21 (m, 2H), 1.66 (m, J = 8.9, 7.4 Hz, 2H), 1.03 (m, J = 7.3, 1.2 Hz, 3H). ^{13}C NMR (101 MHz, $CDCl_3$) δ 133.7, 132.7, 131.7 (d, J = 3.0 Hz), 130.8 (d, J = 9.1 Hz), 128.7 (d, J = 11.1 Hz), 32.2 (d, J = 72.7 Hz), 15.8(d, J = 15.1 Hz), 15.3 (d, J = 3.0 Hz). m.p.: 99-100℃

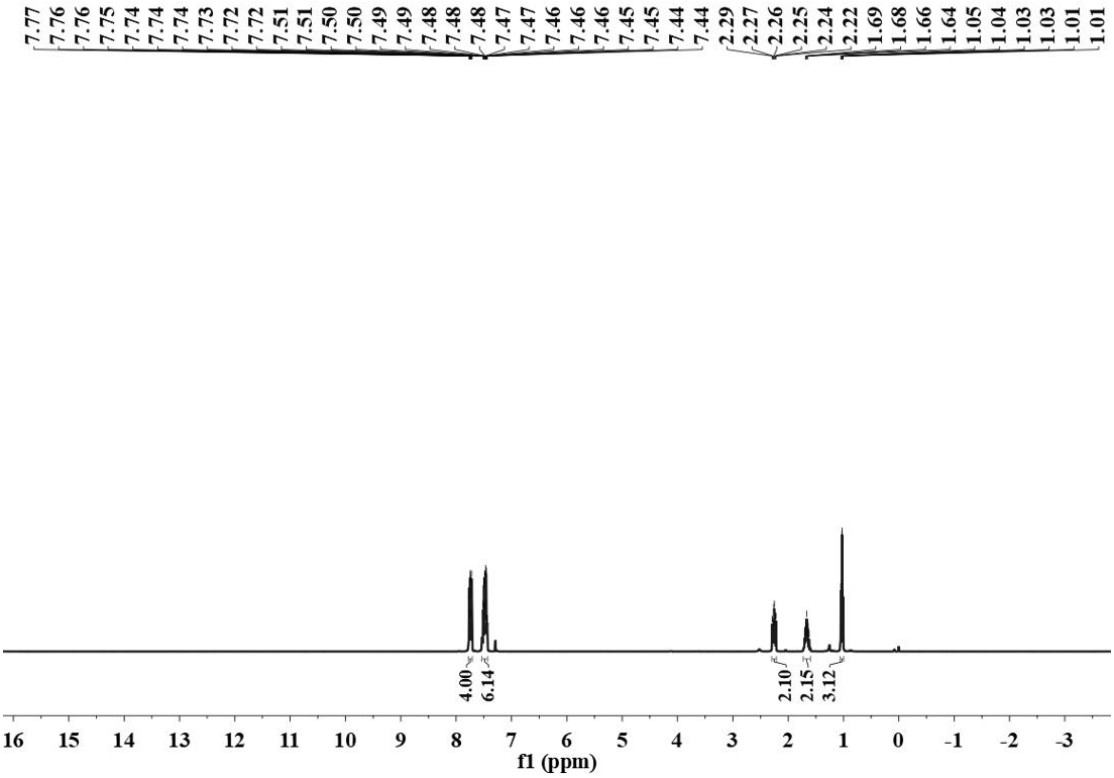

Supplementary Figure 30. ^{1}H NMR spectra of **2k** in $CDCl_3$.

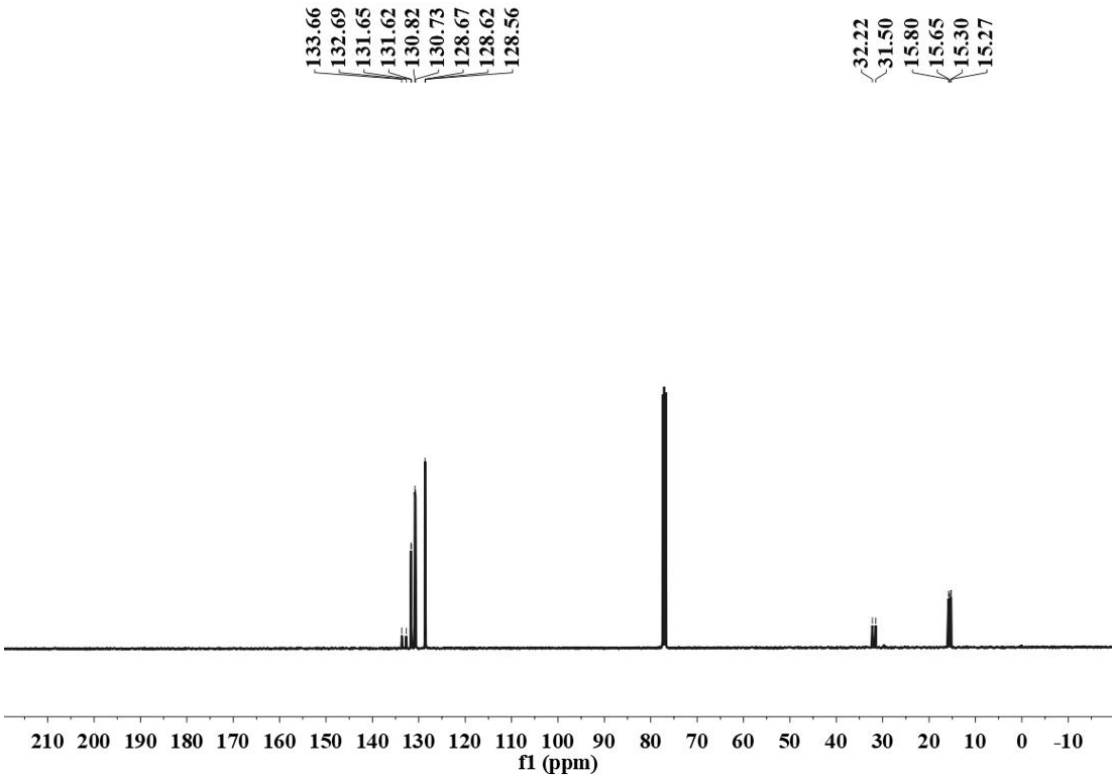

Supplementary Figure 31. ^{13}C NMR spectra of **2k** in $CDCl_3$.

2l. methyldiphenylphosphine oxide[4]

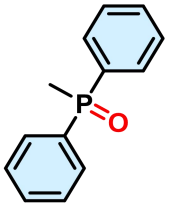

White solid (40.6 mg); 94% yield; eluent: PE/EA = 1:1; ^{1}H NMR (400 MHz, $CDCl_3$) δ 7.80 - 7.68 (m, 4H), 7.60 - 7.41 (m, 6H), 2.03 (d, J = 13.2 Hz, 3H). ^{13}C NMR (101 MHz, $CDCl_3$) δ 134.5, 133.5, 131.8 (d, J = 3.0 Hz), 130.6 (d, J = 5.0 Hz), 128.7 (d, J = 12.1 Hz), 17.0 (d, J = 73.7 Hz). m.p.: 110-112℃.

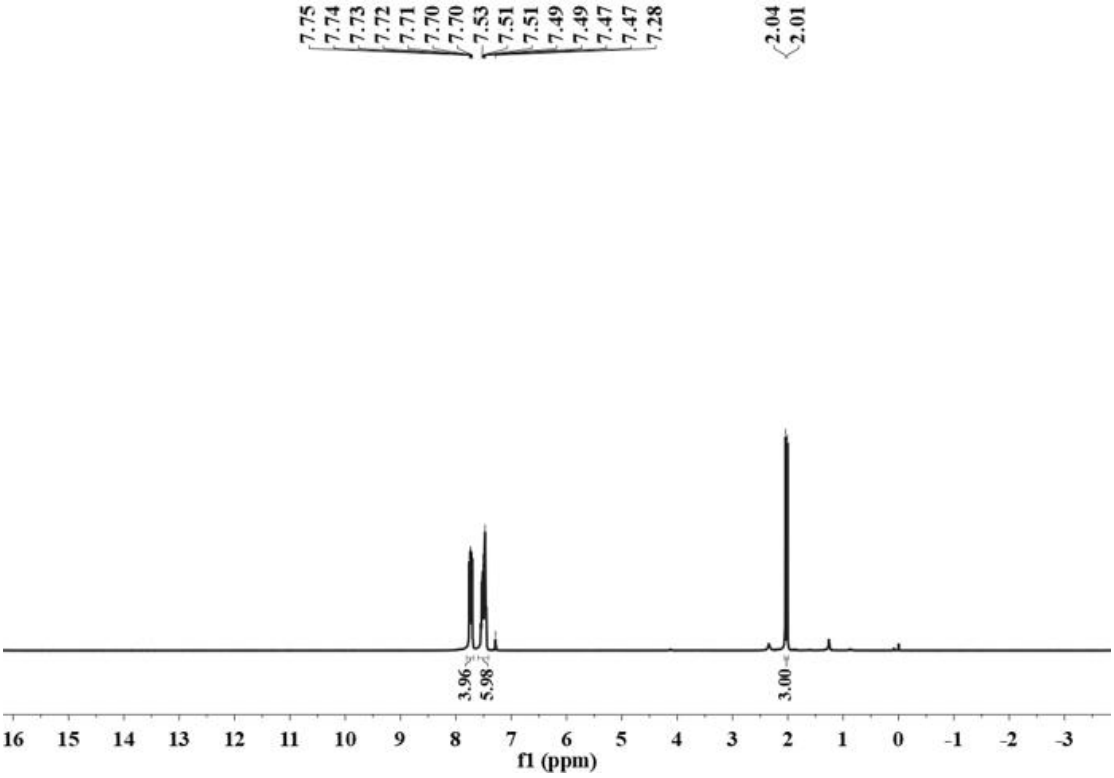

Supplementary Figure 32. ^{1}H NMR spectra of **2l** in $CDCl_3$.

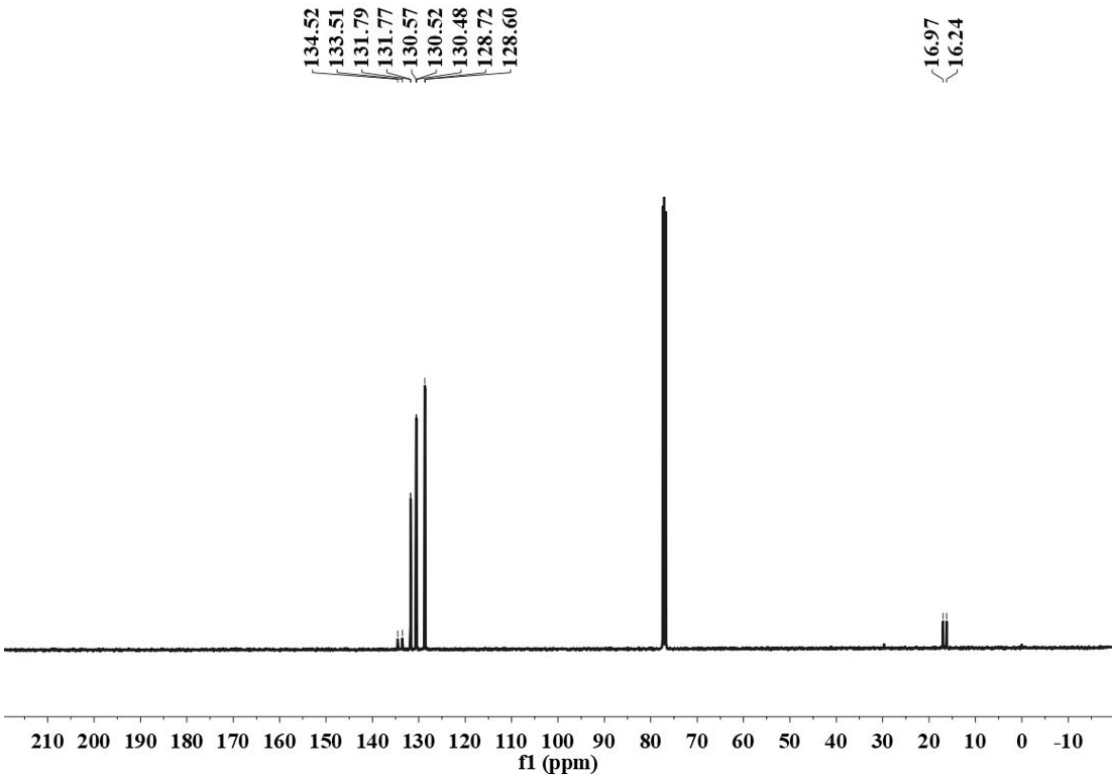

Supplementary Figure 33. ^{13}C NMR spectra of **2l** in $CDCl_3$.

2m. cyclohexyldiphenylphosphine oxide[7]

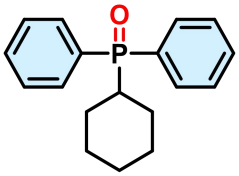

White solid (47.2 mg); 83% yield; eluent: PE/EA = 1:1; ^{1}H NMR (400 MHz, $CDCl_3$) δ 7.78 (m, J = 10.9, 7.8, 1.7 Hz, 4H), 7.59 - 7.42 (m, 6H), 2.24 (m, 1H), 1.81 (m, 2H), 1.77 - 1.67 (m, 3H), 1.55 (dd, J = 10.6, 5.6 Hz, 2H), 1.32 - 1.20 (m, 3H). ^{13}C NMR (101 MHz, $CDCl_3$) δ 132.5, 131.6, 131.4 (d, J = 3.0 Hz), 131.1 (d, J = 8.0 Hz), 128.6, (d, J = 11.1 Hz), 37.5, 36.8, 26.4 (d, J = 13.1 Hz), 25.8, 24.8 (d, J = 3.0 Hz). m.p.: 165 - 167℃.

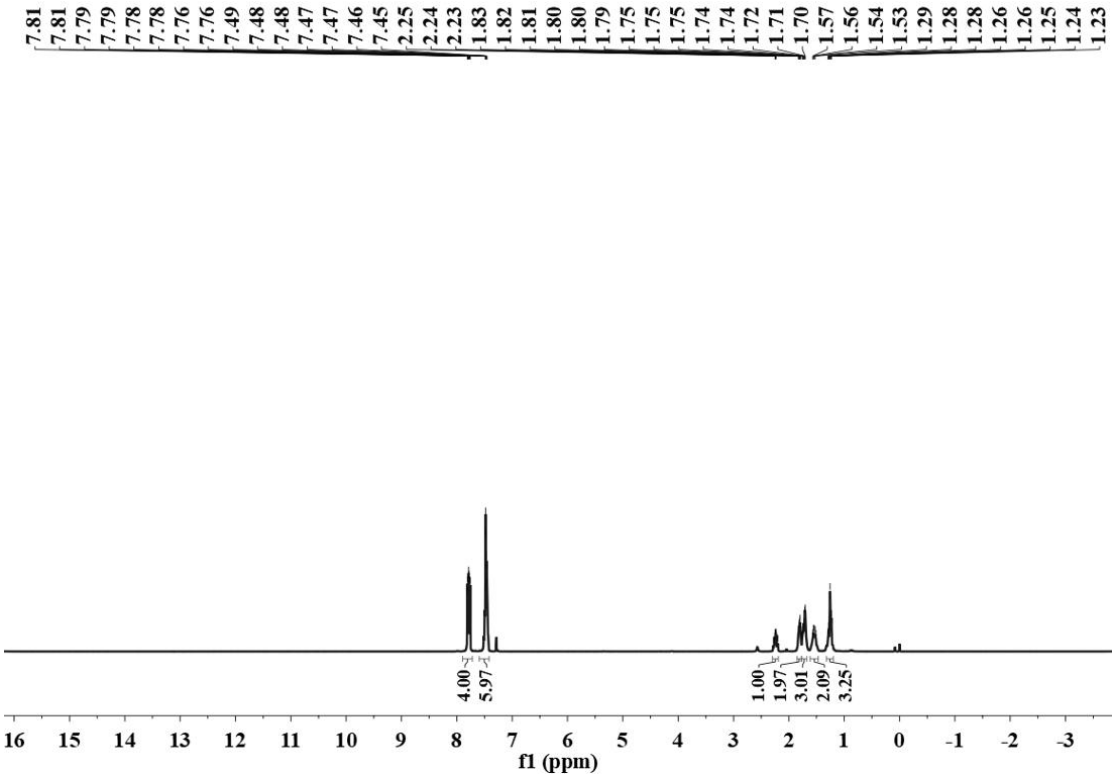

Supplementary Figure 34. ^{1}H NMR spectra of **2m** in $CDCl_3$.

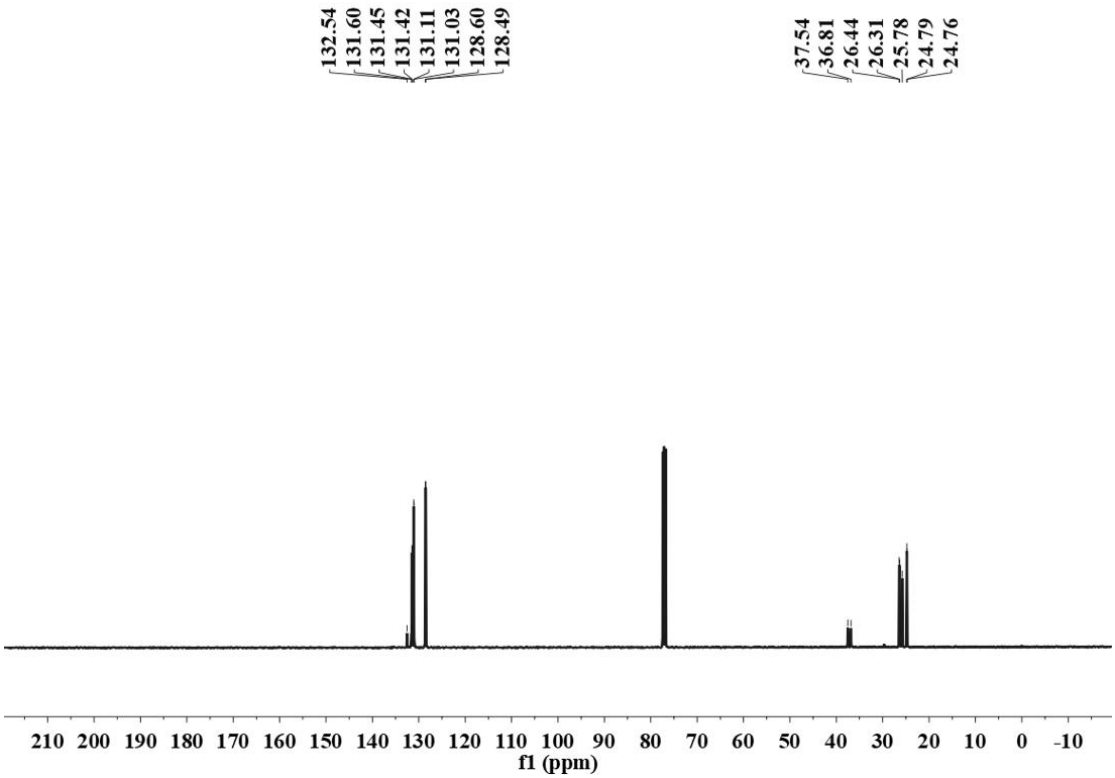

Supplementary Figure 35. ^{13}C NMR spectra of **2m** in $CDCl_3$.

2n. tricyclohexylphosphine oxide[8]

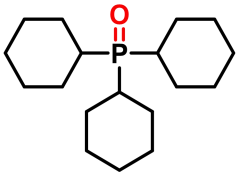

White solid (46.8 mg); 79% yield; eluent: PE/EA = 1:1; ^{1}H NMR (400 MHz, $CDCl_3$) δ 1.96 - 1.64 (m, 18H), 1.47 - 1.16 (m, 15H). ^{13}C NMR (101 MHz, $CDCl_3$) δ 35.6, 35.0, 27.0 (d, J = 12.1 Hz), 26.3(d, J = 3.0 Hz), 26.1(d, J = 1.0 Hz). m.p.: 155-157°C

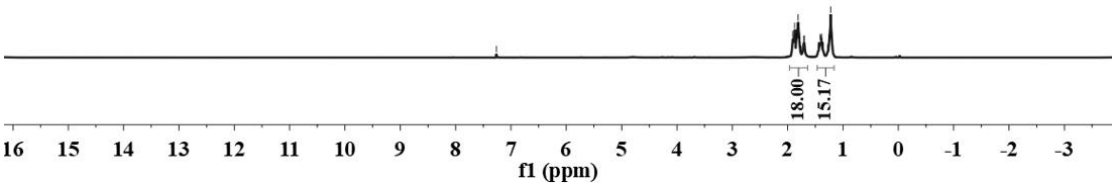

Supplementary Figure 36. ^{1}H NMR spectra of **2n** in $CDCl_3$.

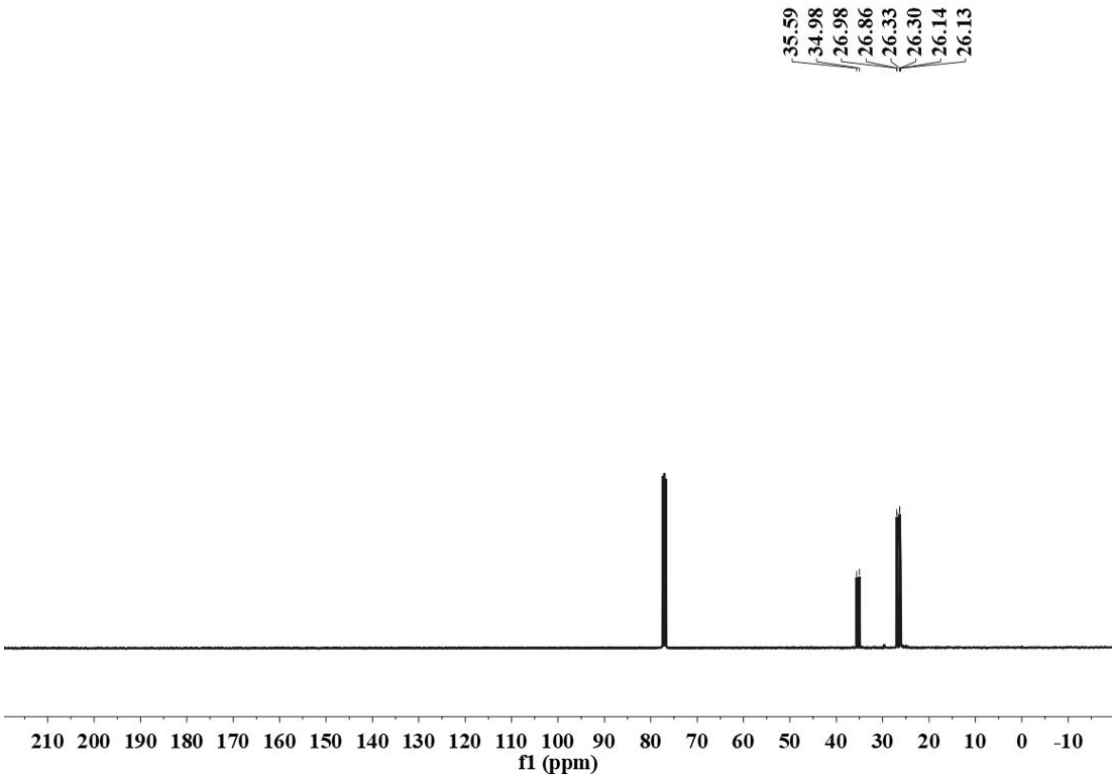

Supplementary Figure 37. ^{13}C NMR spectra of **2n** in $CDCl_3$.

2o. propane-1,3-diylbis(diphenylphosphine oxide) [8]

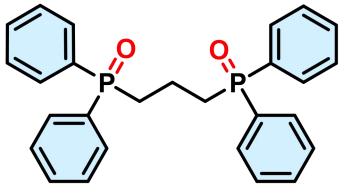

White solid (71.0 mg); 80% yield; eluent: PE/EA = 1:1; ^{1}H NMR (400 MHz, $CDCl_3$) δ 7.73 - 7.65 (m, 8H), 7.51 - 7.39 (m, 12H), 2.51 (m, 4H). ^{13}C NMR (101 MHz, $CDCl_3$) δ 133.0, 132.1, 131.8 (d, J = 2.0 Hz), 130.7 (d, J = 9.1 Hz), 128.7 (d, J = 12.1 Hz), 30.4 (d, J = 10.9 Hz), 29.7 (d, J = 11.0 Hz), 14.9 (t, J = 3.6 Hz). m.p.: 268-269°C

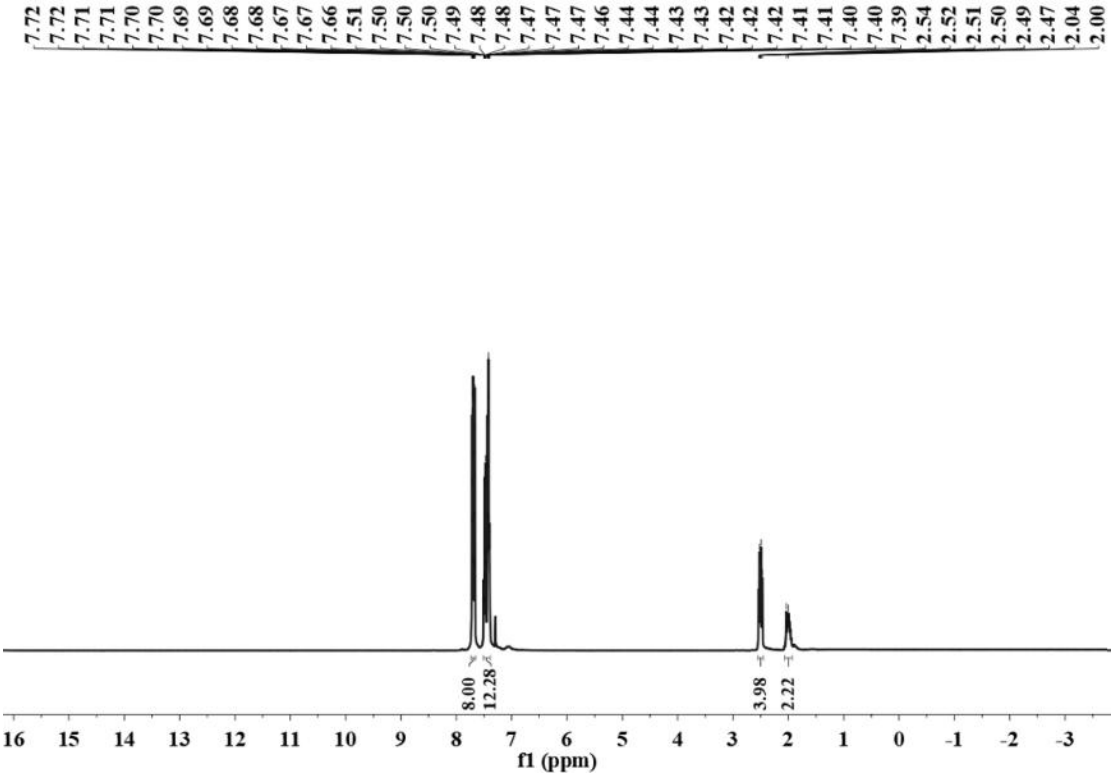

Supplementary Figure 38. ^{1}H NMR spectra of **2o** in $CDCl_3$.

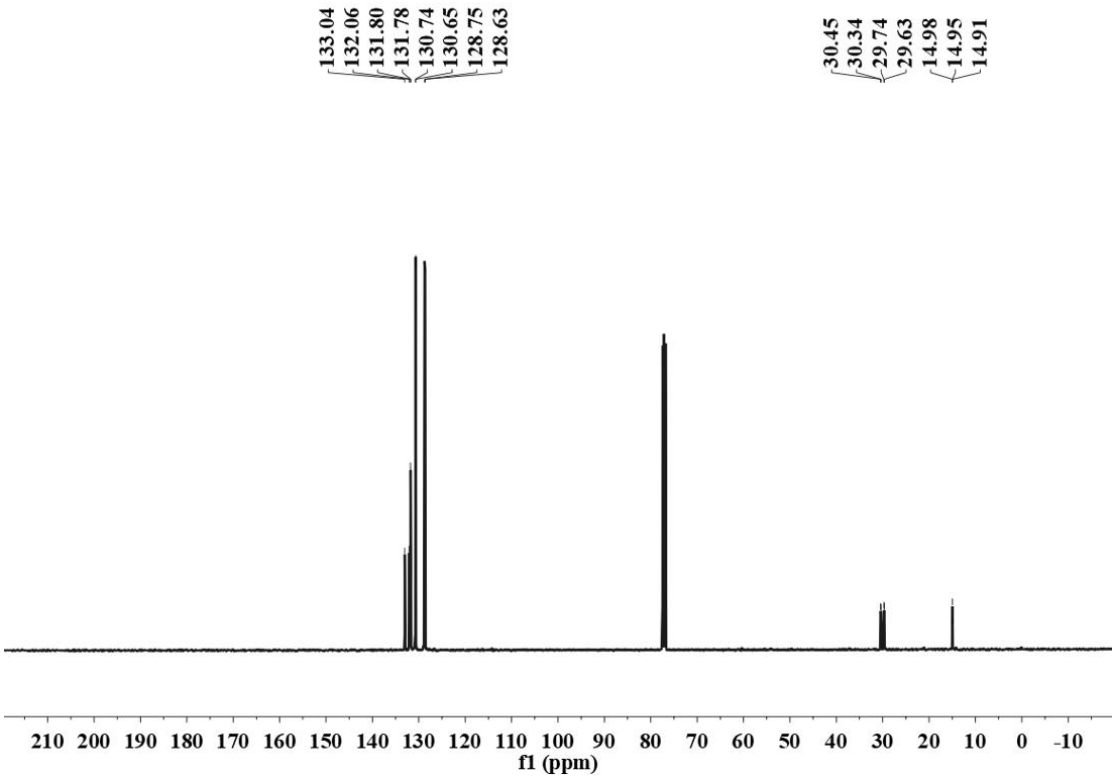

Supplementary Figure 39. ^{13}C NMR spectra of **2o** in $CDCl_3$.

^{1}H NMR spectra and data of 4a-4i

4a. 1-(1H-indol-3-yl)-2-phenyl-1,2,3,4-tetrahydroisoquinoline[9]

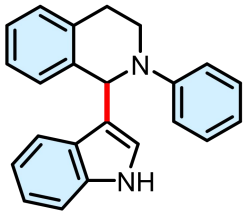

White solid (27.5 mg); 85% yield; eluent: PE/EA = 20:1; ^{1}H NMR (400 MHz, $CDCl_3$) δ 7.90 (s, 1H), 7.55 (d, J = 7.8 Hz, 1H), 7.39 - 7.27 (m, 2H), 7.26 - 7.14 (m, 6H), 7.02 (d, J = 7.9 Hz, 3H), 6.77 (t, J = 7.4 Hz, 1H), 6.61 (s, 1H), 6.17 (s, 1H), 3.62 (t, J = 6.3 Hz, 2H), 3.06 (dt, J = 15.8, 7.7 Hz, 1H), 2.86 - 2.74 (m, 1H). ^{13}C NMR (101 MHz, $CDCl_3$) δ 149.79, 137.41, 136.60, 135.59, 129.24, 128.85, 128.07, 126.70, 126.45, 125.73, 124.22, 122.12, 120.10, 119.64, 119.24, 118.12, 115.82, 111.09, 56.65, 42.30, 26.63. m.p.: 179-180°C.

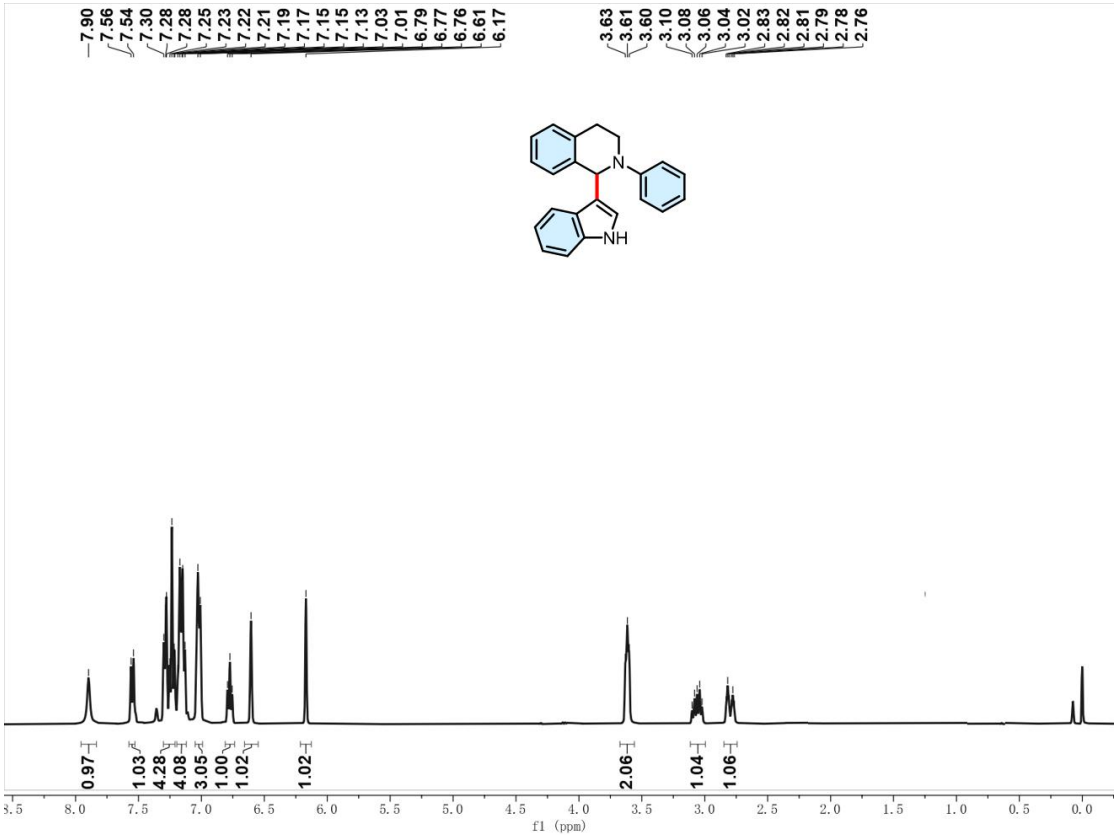

Supplementary Figure 40. ^{1}H NMR spectra of **4a** in $CDCl_3$.

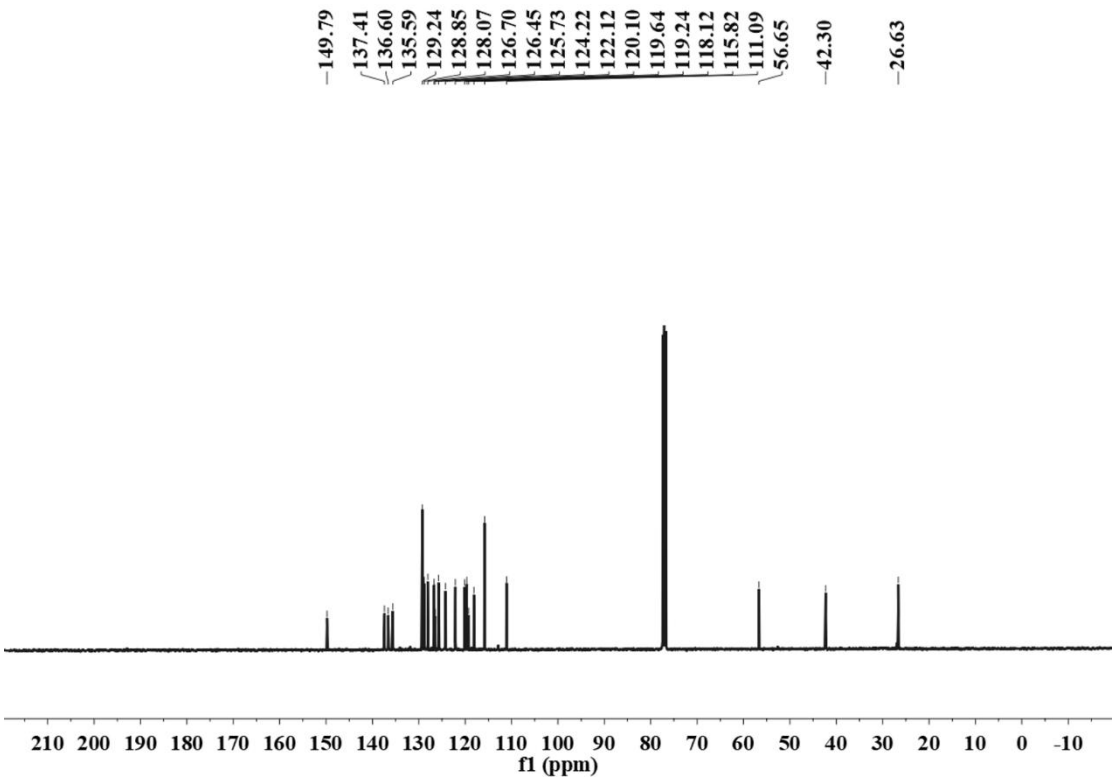

Supplementary Figure 41. ^{13}C NMR spectra of **4a** in $CDCl_3$.

4b. 2-(4-fluorophenyl)-1-(1H-indol-3-yl)-1,2,3,4-tetrahydroisoquinoline[9]

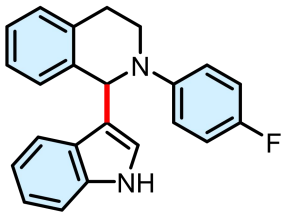

White solid (28.0 mg); 82% yield; eluent: PE/EA = 20:1; ^{1}H NMR (400 MHz, $CDCl_3$) δ 7.90 (s, 1H), 7.55 (d, *J* = 7.8 Hz, 1H), 7.39 - 7.27 (m, 2H), 7.26 - 7.14 (m, 6H), 7.02 (d, *J* = 7.9 Hz, 3H), 6.77 (t, *J* = 7.4 Hz, 1H), 6.61 (s, 1H), 6.17 (s, 1H), 3.62 (t, *J* = 6.3 Hz, 2H), 3.06 (dt, *J* = 15.8, 7.7 Hz, 1H), 2.86 - 2.74 (m, 1H). ^{13}C NMR (101 MHz, $CDCl_3$) δ 157.84 (d, *J* = 238.3 Hz), 146.82, 137.24, 136.49, 135.27, 128.88, 128.14, 126.67, 126.59, 125.81, 124.28, 122.12, 120.06, 119.66, 118.95 (d, *J* = 23.2 Hz), 118.65, 115.61(d, *J* = 22.2 Hz), 111.06, 57.67, 43.45, 26.78. m.p.: 164 - 165°C.

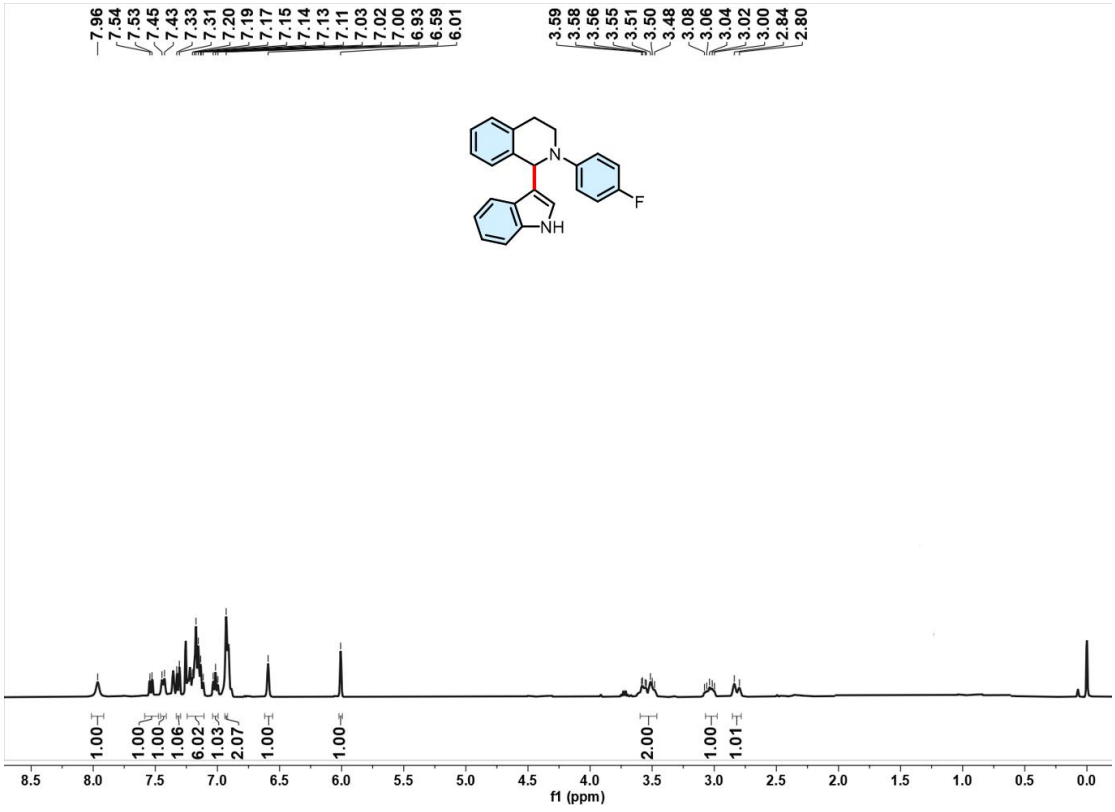

Supplementary Figure 42. ^{1}H NMR spectra of **4b** in $CDCl_3$.

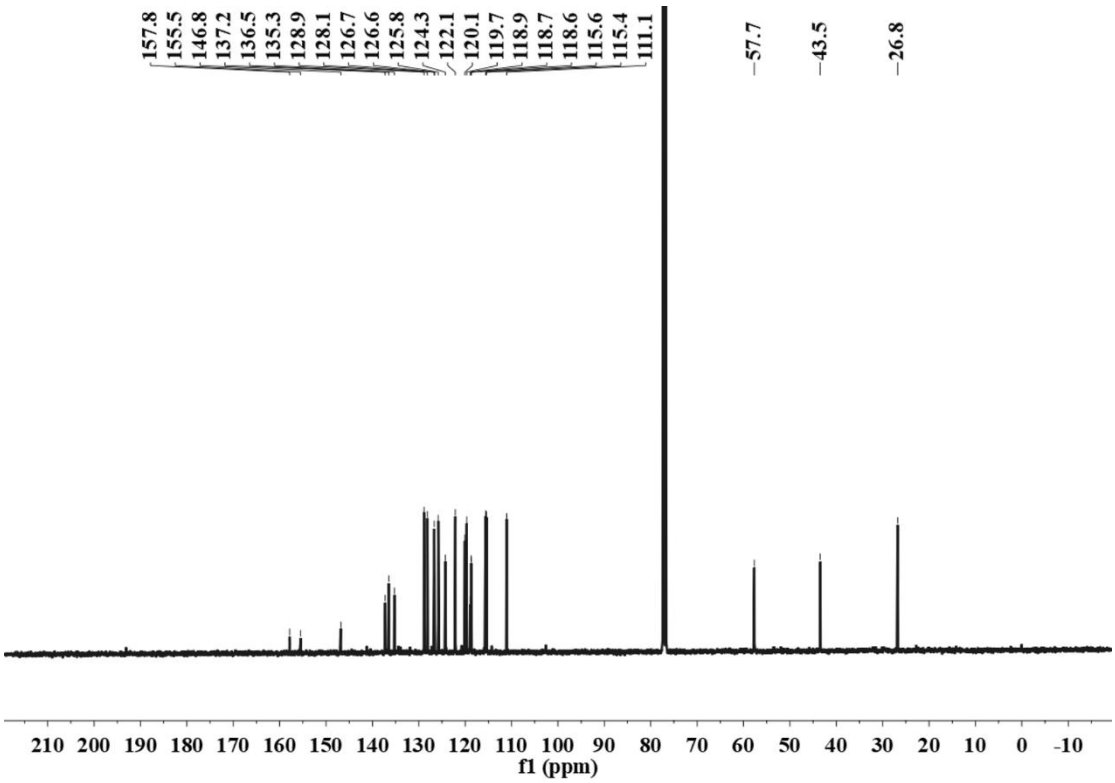

Supplementary Figure 43. ^{13}C NMR spectra of **4b** in $CDCl_3$.

4c. 1-(1H-indol-3-yl)-2-(4-chlorine)-1,2,3,4-tetrahydroisoquinoline[9]

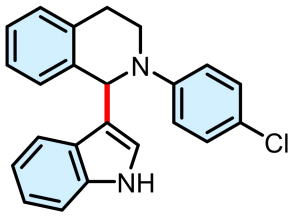

White solid (30.0 mg); 84% yield; eluent: PE/EA = 20:1; ^{1}H NMR (400 MHz, $CDCl_3$) δ 7.83 (s, 1H), 7.33 - 7.27 (m, 2H), 7.24 - 7.21 (m, 2H), 7.16 (m, J = 13.2, 8.9, 5.7, 3.5 Hz, 4H), 7.05 - 6.98 (m, 3H), 6.81 - 6.76 (m, 1H), 6.57 (dd, J = 2.5, 1.0 Hz, 1H), 6.13 (s, 1H), 3.65 - 3.61 (m, 2H), 3.11 - 3.02 (m, 1H), 2.83 - 2.77 (m, 1H), 2.37 (s, 3H). ^{13}C NMR (101 MHz, $CDCl_3$) δ 148.73, 137.01, 136.61, 135.33, 131.93, 128.84, 127.99, 126.92, 126.89, 126.27, 125.88, 124.13, 122.24, 119.91, 119.75, 118.82, 117.26, 111.17, 109.93, 56.63, 42.50, 26.62. m.p.: 69-70°C.

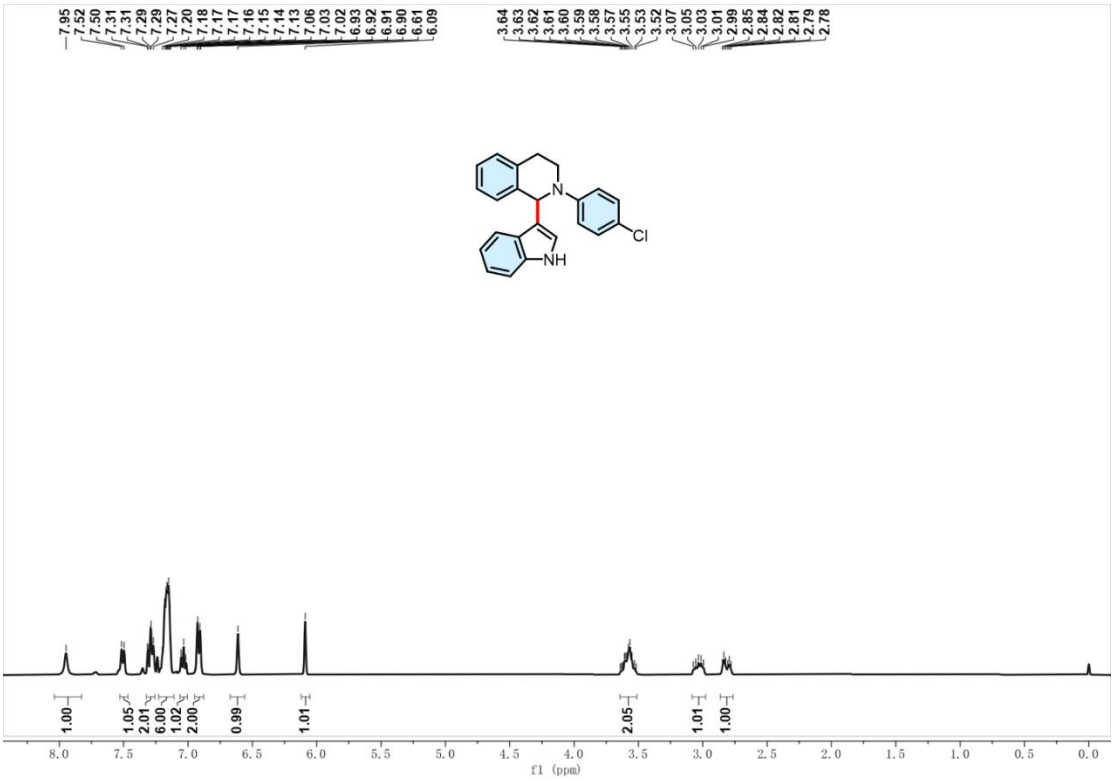

Supplementary Figure 44. ^{1}H NMR spectra of **4c** in $CDCl_3$.

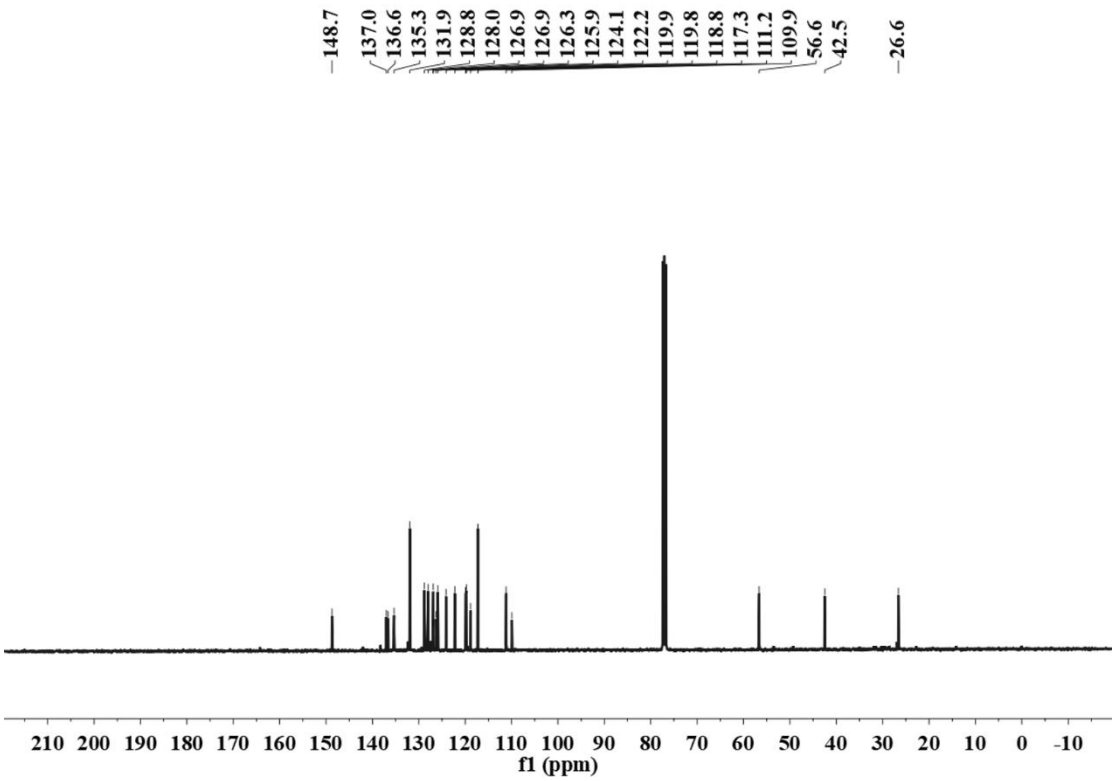

Supplementary Figure 45. ^{13}C NMR spectra of **4c** in $CDCl_3$.

4d. 1-(1H-indol-3-yl)-2-(4- bromine)-1,2,3,4-tetrahydroisoquinoline[9]

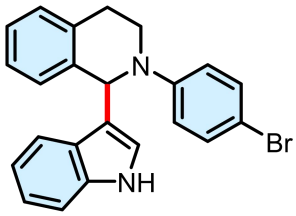

White solid (33.0 mg); 82% yield; eluent: PE/EA = 20:1; ^{1}H NMR (400 MHz, $CDCl_3$) δ 7.98 (s, 1H), 7.52 (d, J = 8.2 Hz, 1H), 7.33 - 7.28 (m, 4H), 7.22 - 7.14 (m, 4H), 7.06 - 7.00 (m, 1H), 6.90 (s, 1H), 6.68 - 6.64 (m, 1H), 6.11 (s, 1H), 3.63 - 3.56 (m, 2H), 3.07 - 3.01 (m, 1H), 2.86 - 2.80 (m, 1H). ^{13}C NMR (101 MHz, $CDCl_3$) δ 148.40, 137.07, 136.60, 135.33, 129.04, 128.86, 128.03, 126.87, 126.32, 125.88, 124.17, 122.84, 122.22, 119.92, 119.74, 118.83, 117.00, 111.18, 56.77, 42.61, 26.65. m.p.: 68-69°C.

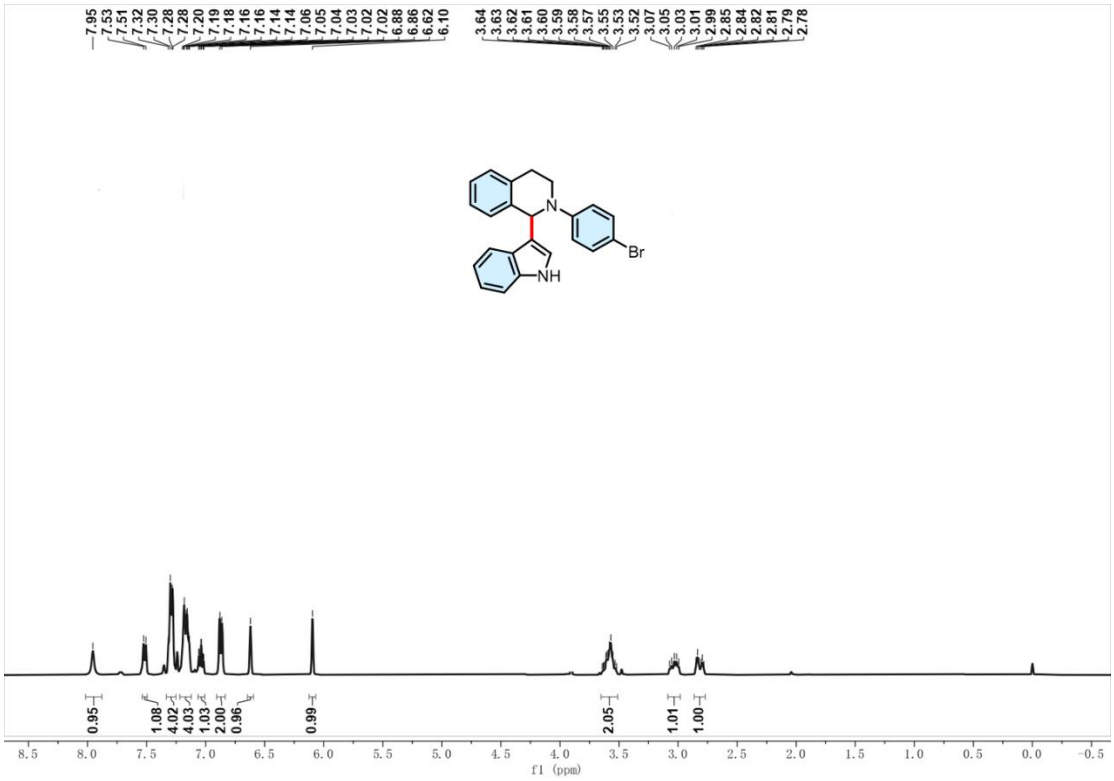

Supplementary Figure 46. ^{1}H NMR spectra of **4d** in $CDCl_3$.

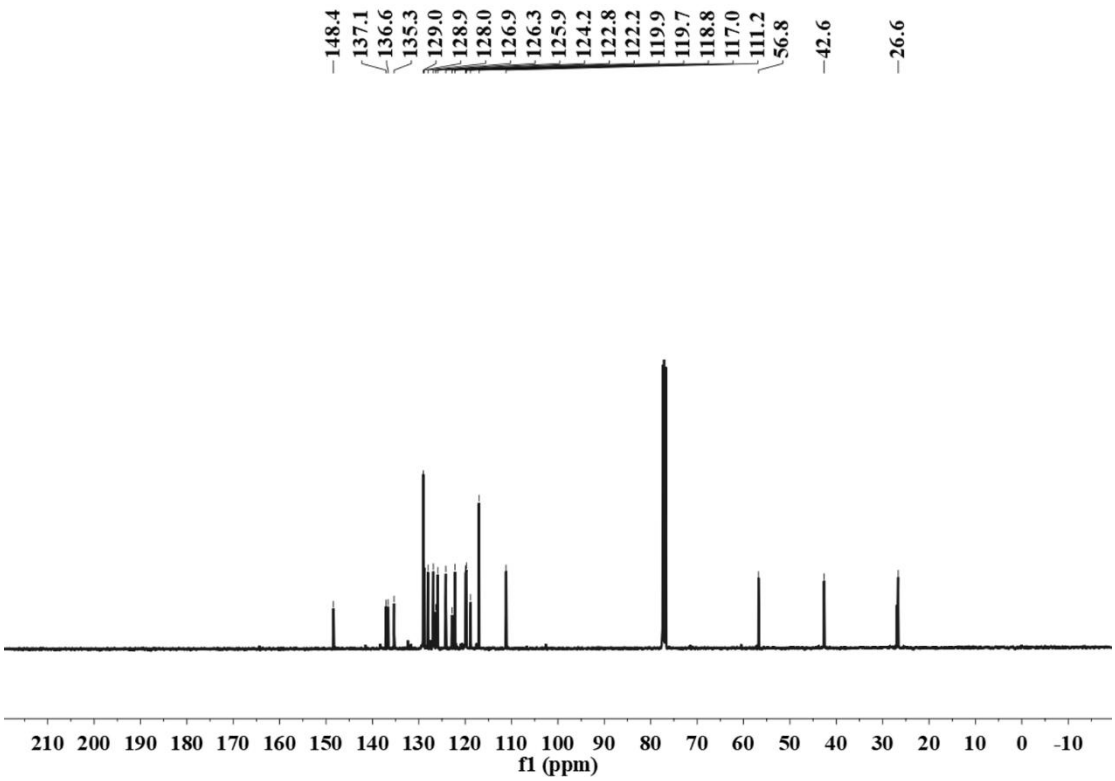

Supplementary Figure 47. ^{13}C NMR spectra of **4d** in $CDCl_3$.

4e. 2-(4-methoxy)-1-(1H-indol-3-yl)-1,2,3,4-tetrahydroisoquinoline[9]

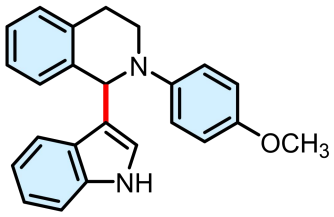

White solid (25.1 mg); 71% yield; eluent: PE/EA = 20:1; ^{1}H NMR (400 MHz, $CDCl_3$) δ 7.94 (s, 1H), 7.42 (d, J = 8.1 Hz, 1H), 7.31 (d, J = 8.2 Hz, 1H), 7.18 (q, J = 12.3, 9.8 Hz, 5H), 7.01 - 6.91 (m, 3H), 6.82 - 6.75 (m, 2H), 6.57 (s, 1H), 5.96 (s, 1H), 3.76 - 3.73 (m, 3H), 3.57 - 3.44 (m, 2H), 3.03 (d, J = 7.5 Hz, 1H), 2.80 (d, J = 16.6 Hz, 1H). ^{13}C NMR (101 MHz, $CDCl_3$) δ 153.53, 145.35, 135.78, 134.60, 134.55, 128.74, 127.85, 126.57, 126.32, 125.96, 124.19, 121.96, 120.73, 119.79, 118.14, 114.58, 111.06, 55.67, 52.75, 48.54, 29.13. m.p.: 162-163°C.

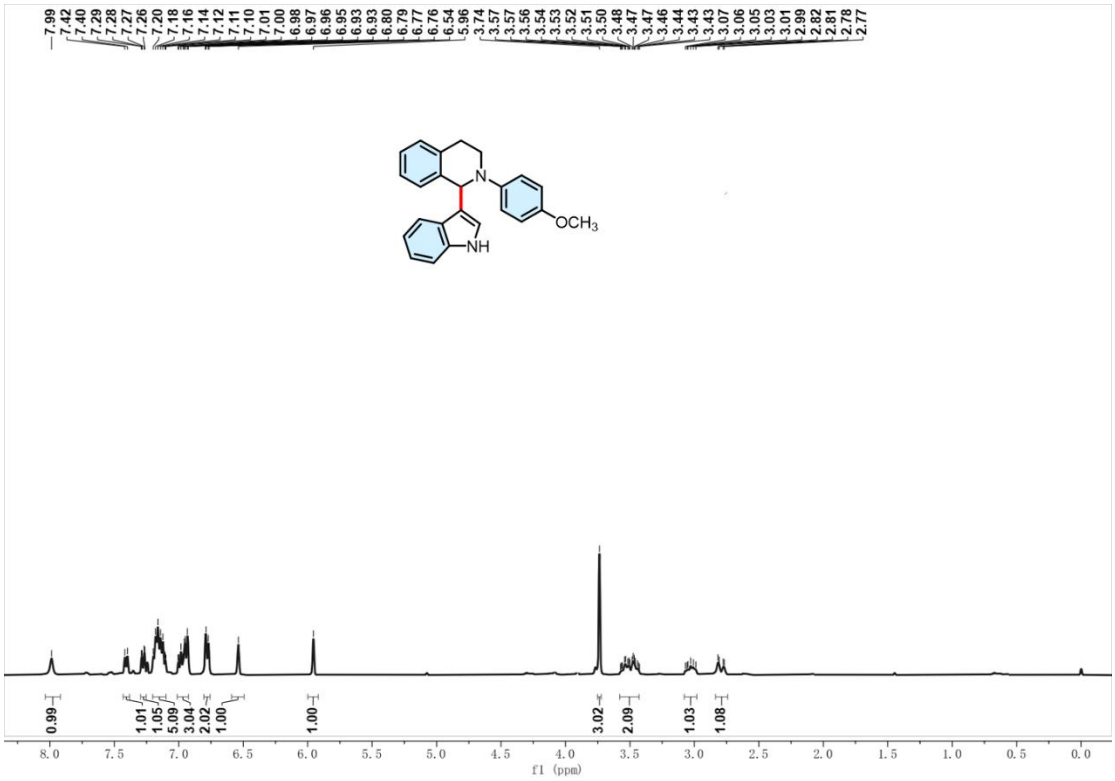

Supplementary Figure 48. ^{1}H NMR spectra of **4e** in $CDCl_3$.

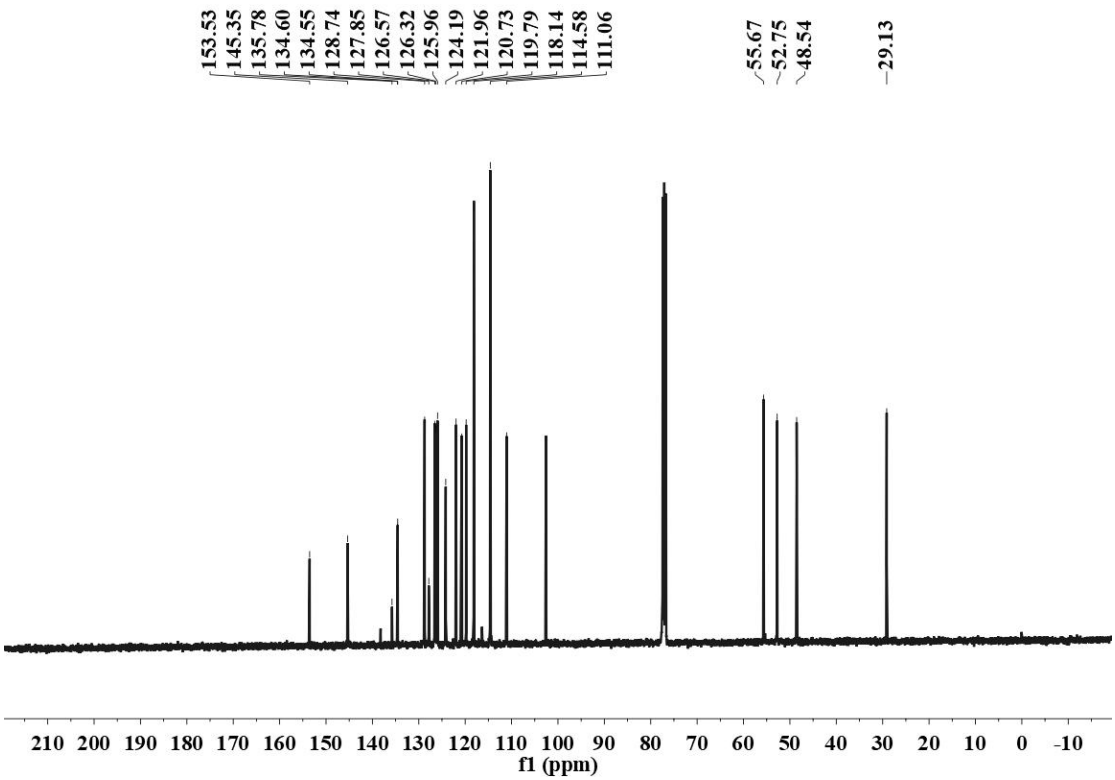

Supplementary Figure 49. ^{13}C NMR spectra of **4e** in $CDCl_3$.

4f. 1-(4-fluoro-1h-indole-3-yl)-2-phenyl-1,2,3,4-tetrahydroisoquinoline[10]

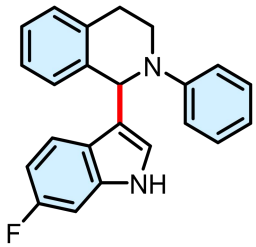

White solid (26.6 mg); 78% yield; eluent: PE/EA = 20:1; ^{1}H NMR (400 MHz, $CDCl_3$) δ 7.94 (s, 1H), 7.42 (d, J = 8.1 Hz, 1H), 7.31 (d, J = 8.2 Hz, 1H), 7.18 (q, J = 12.3, 9.8 Hz, 5H), 7.01 - 6.91 (m, 3H), 6.82 - 6.75 (m, 2H), 6.57 (s, 1H), 5.96 (s, 1H), 3.76 - 3.73 (m, 3H), 3.57 - 3.44 (m, 2H), 3.03 (d, J = 7.5 Hz, 1H), 2.80 (d, J = 16.6 Hz, 1H). ^{13}C NMR (101 MHz, $CDCl_3$) δ 161.09, 158.72, 149.77, 137.10, 136.59 (d, *J* = 12.1 Hz), 135.53, 129.27, 128.94, 128.01, 126.79, 125.73, 124.52 (d, *J* = 3.0 Hz), 123.08, 121.00 (d, *J* = 10.1 Hz), 119.41, 118.40, 116.06, 108.51 (d, *J* = 24.2 Hz), 97.42 (d, *J* = 26.2 Hz), 56.62, 42.29, 26.53. m.p.: 175-176°C.

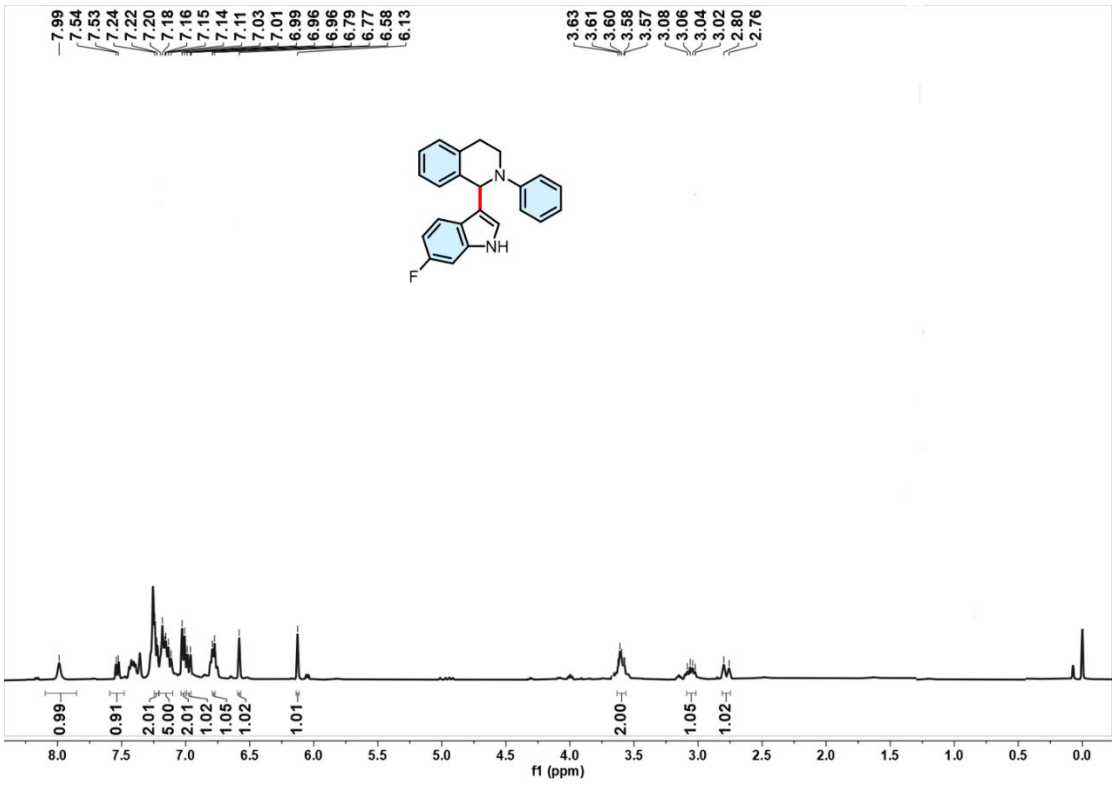

Supplementary Figure 50. ^{1}H NMR spectra of **4f** in $CDCl_3$.

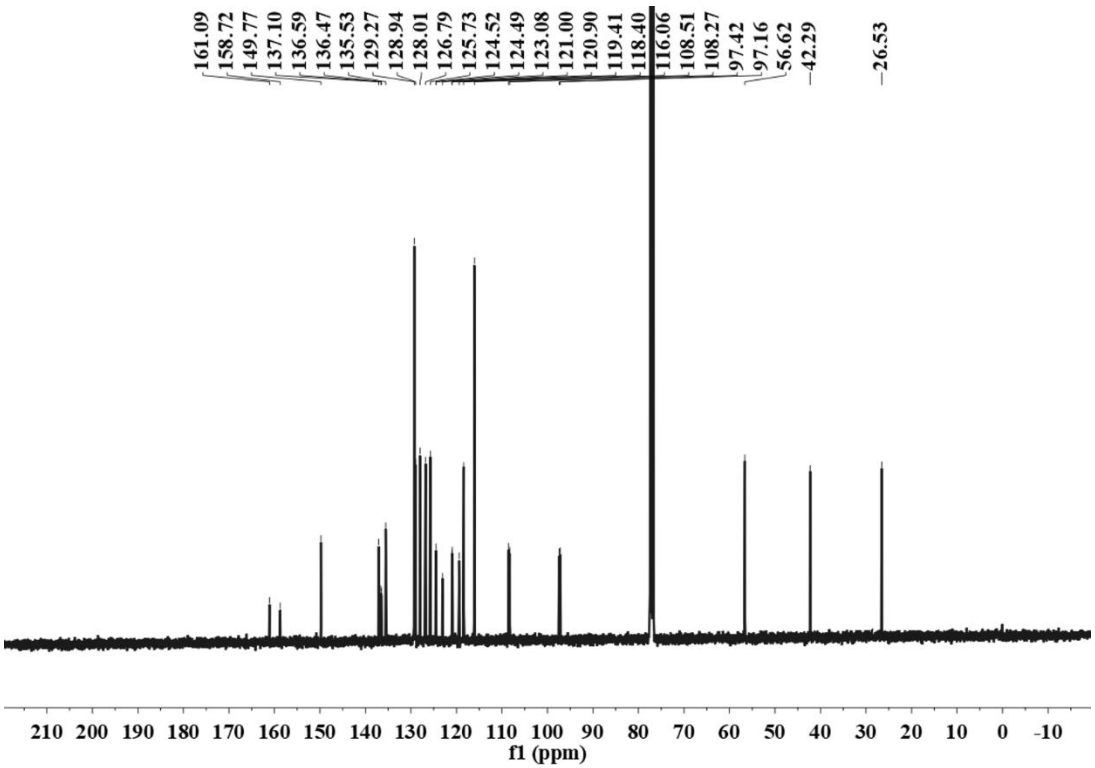

Supplementary Figure 51. ^{13}C NMR spectra of **4f** in $CDCl_3$.

4g. 1-(6-chloro-1H-indol-3-yl)-2-phenyl-1,2,3,4-tetrahydroisoquinoline[9]

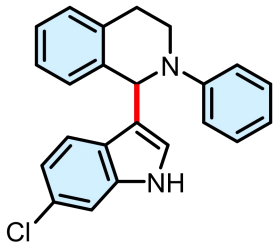

White solid (27.2 mg); 76% yield; eluent: PE/EA = 20:1; ^{1}H NMR (400 MHz, $CDCl_3$) δ 7.99 (s, 1H), 7.59 - 7.48 (m, 1H), 7.24 - 7.20 (m, 2H), 7.20 - 7.07 (m, 5H), 7.02 (d, *J* = 8.0 Hz, 2H), 6.97 (d, *J* = 9.6 Hz, 1H), 6.77 (s, 1H), 6.58 (s, 1H), 6.13 (s, 1H), 3.63 - 3.56 (m, 2H), 3.05 (d, *J* = 8.2 Hz, 1H), 2.78 (d, *J* = 16.2 Hz, 1H). ^{13}C NMR (101 MHz, $CDCl_3$) δ 149.79, 137.05, 136.93, 135.50, 129.27, 128.95, 128.04, 127.97, 126.83, 125.78, 125.07, 124.80, 121.06, 120.38, 119.43, 118.52, 116.18, 110.95, 56.64, 42.37, 26.94, 26.63. m.p.: 177 - 178°C.

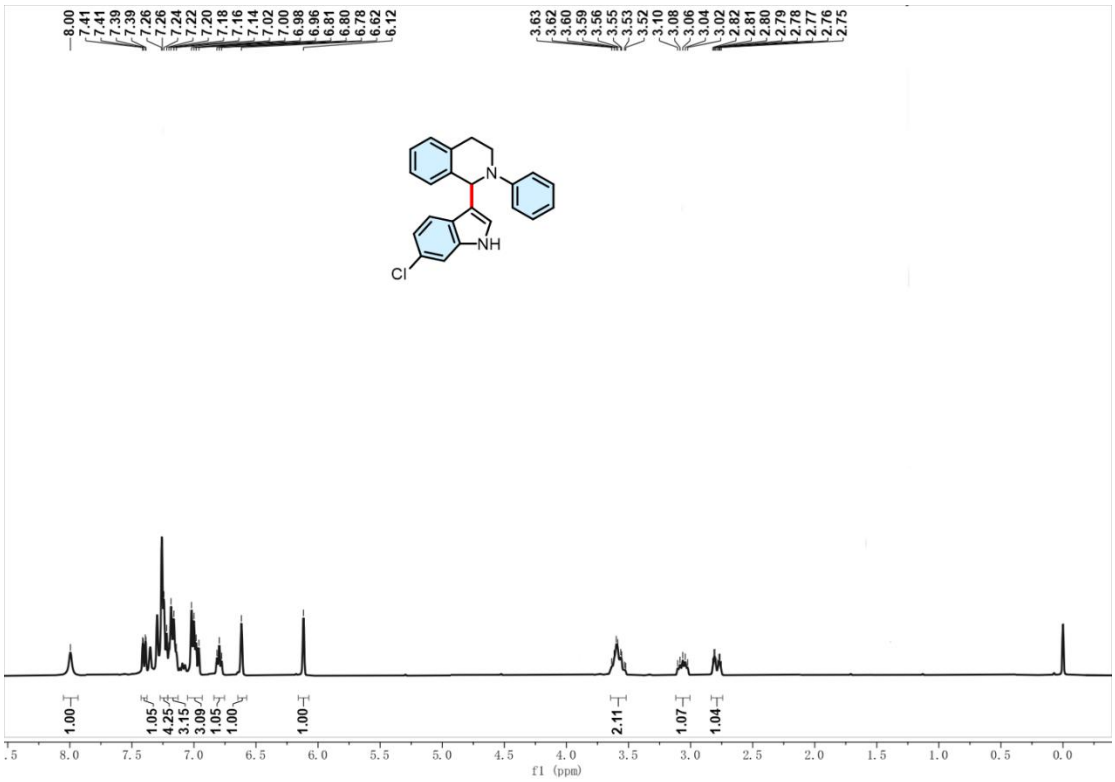

Supplementary Figure 52. ^{1}H NMR spectra of **4g** in $CDCl_3$.

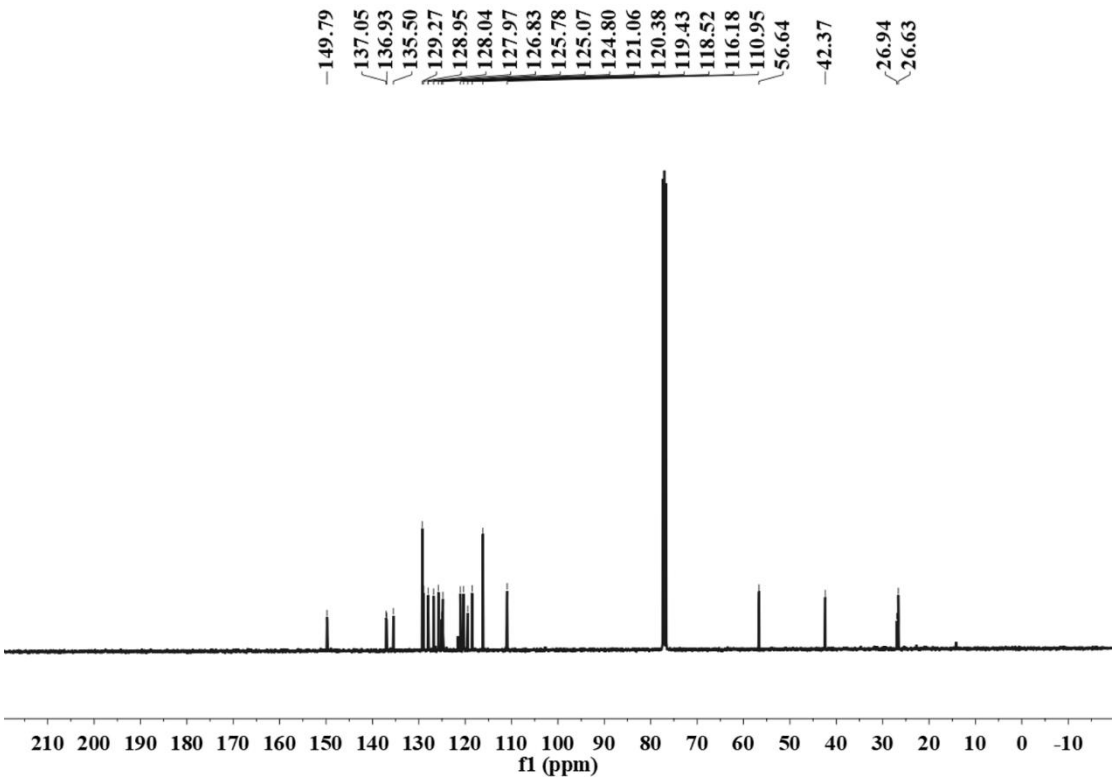

Supplementary Figure 53. ^{13}C NMR spectra of **4g** in $CDCl_3$.

4h. 1-(6-bromo-1H-indol-3-yl)-2-phenyl-1,2,3,4-tetrahydroisoquinoline[10]

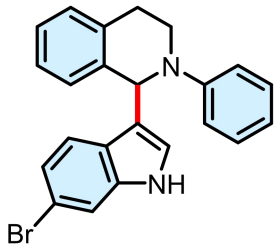

White solid (28.0 mg); 70% yield; eluent: PE/EA = 20:1; ^{1}H NMR (400 MHz, $CDCl_3$) δ 8.02 (s, 1H), 7.53 (dd, J = 8.6, 2.1 Hz, 1H), 7.23 (s, 3H), 7.20 - 7.14 (m, 4H), 6.99 (dd, J = 16.2, 8.4 Hz, 3H), 6.80 (t, J = 7.2 Hz, 1H), 6.62 (s, 1H), 6.12 (s, 1H), 3.67 - 3.56 (m, 2H), 3.07 (dd, J = 16.2, 7.9 Hz, 1H), 2.82 - 2.75 (m, 1H); ^{13}C NMR (101 MHz, $CDCl_3$) δ 149.79, 137.35, 137.04, 135.48, 129.27, 128.95, 127.96, 126.84, 125.79, 125.37, 124.80, 124.74, 123.13, 122.94, 121.94, 121.43, 119.45, 118.54, 116.21, 115.70, 113.95, 56.64, 42.39, 26.66. m.p.: 178 - 179°C.

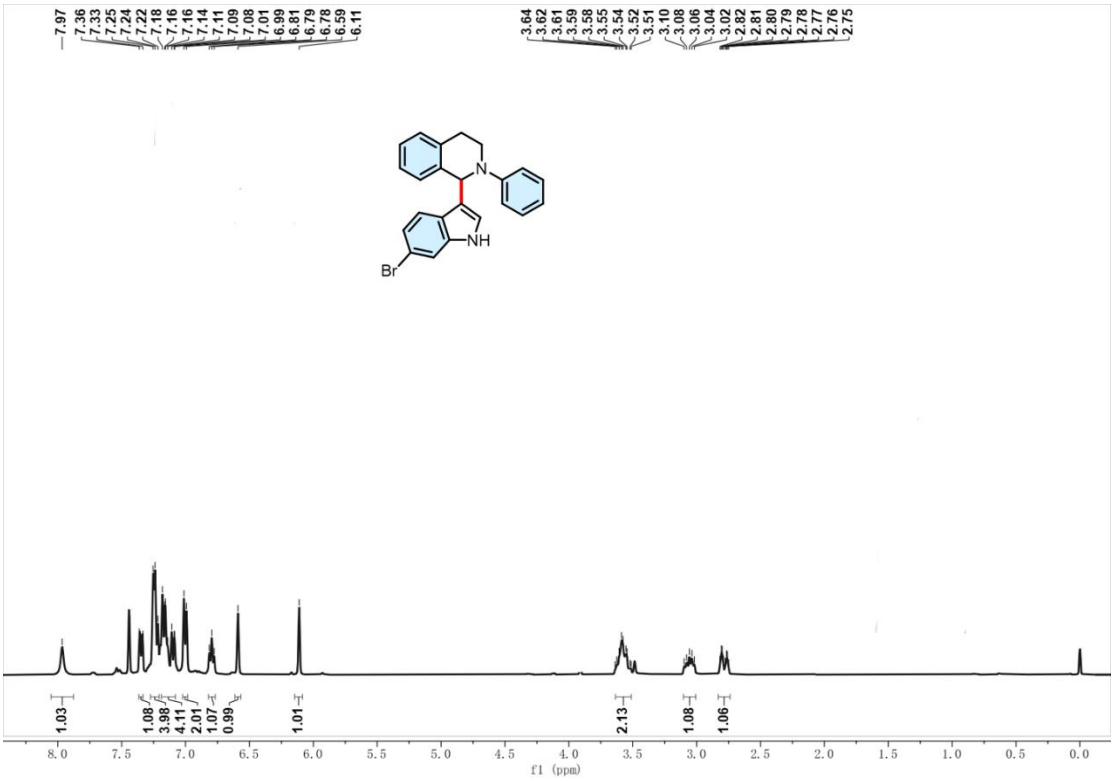

Supplementary Figure 54. ^{1}H NMR spectra of **4h** in $CDCl_3$.

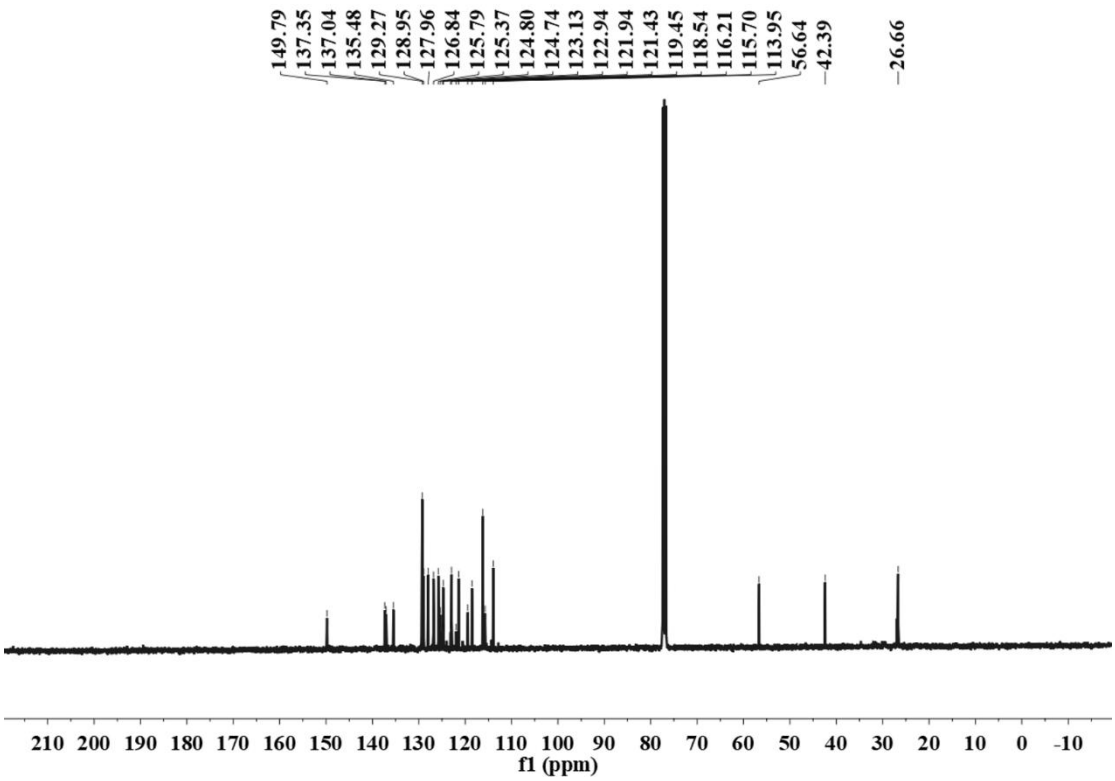

Supplementary Figure 55. ^{13}C NMR spectra of **4h** in $CDCl_3$.

4i. 1-(5-methoxy-1H-indol-3-yl)-2-phenyl-1,2,3,4-tetrahydroisoquinoline[9]

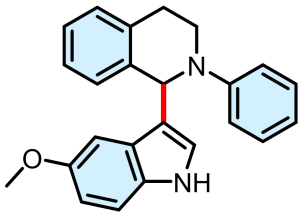

White solid (24.0 mg); 68% yield; eluent: PE/EA = 20:1; ^{1}H NMR (400 MHz, $CDCl_3$) δ 7.67 (s, 1H), 7.16 (s, 5H), 7.08 - 7.03 (m, 3H), 7.00 (dd, J = 8.4, 2.5 Hz, 3H), 6.89 (td, J = 7.7, 1.9 Hz, 1H), 6.82 (t, J = 7.4 Hz, 1H), 5.96 (s, 1H), 3.68 - 3.57 (m, 2H), 3.11 - 2.95 (m, 2H). ^{13}C NMR (101 MHz, $CDCl_3$) δ 154.18, 153.86, 150.02, 137.52, 135.57, 131.60, 130.93, 129.22, 128.81, 128.27, 128.02, 126.92, 126.71, 125.70, 125.03, 124.87, 118.69, 118.31, 116.22, 112.36, 112.26, 111.72, 111.68, 102.40, 102.26, 101.86, 56.88, 55.86, 55.70, 42.13, 26.95. m.p.: 172-174°C.

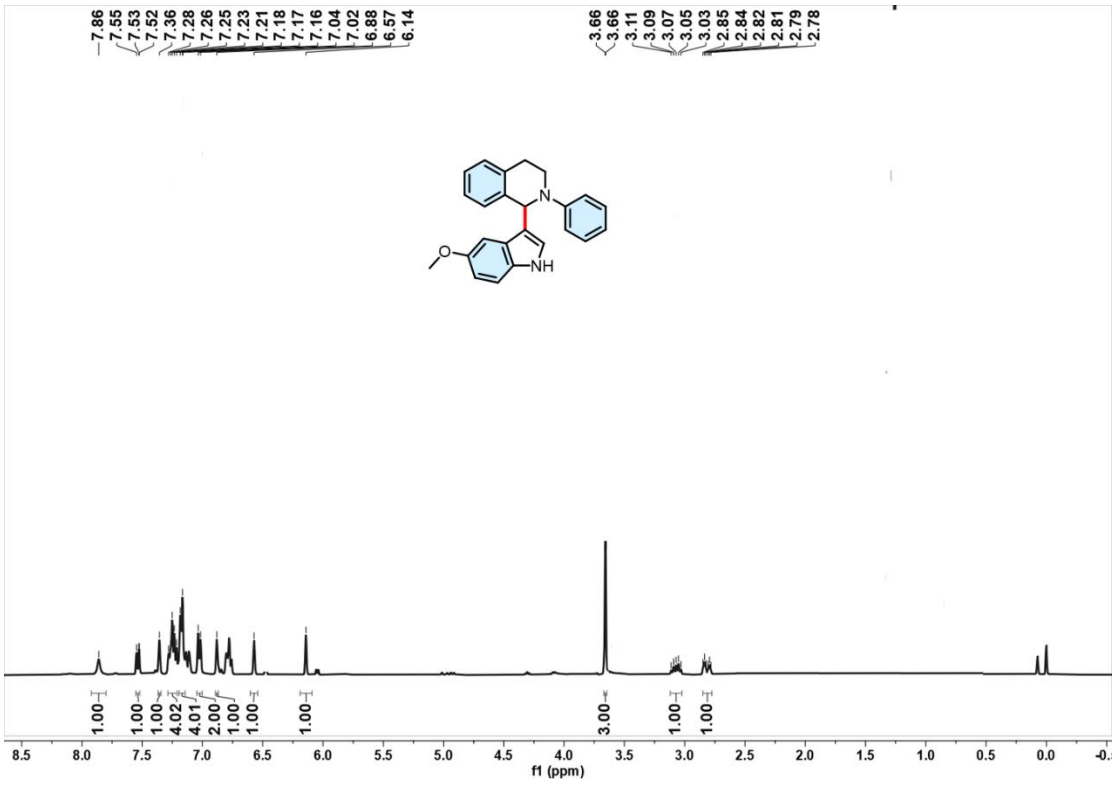

Supplementary Figure 56. ^{1}H NMR spectra of **4i** in $CDCl_3$.

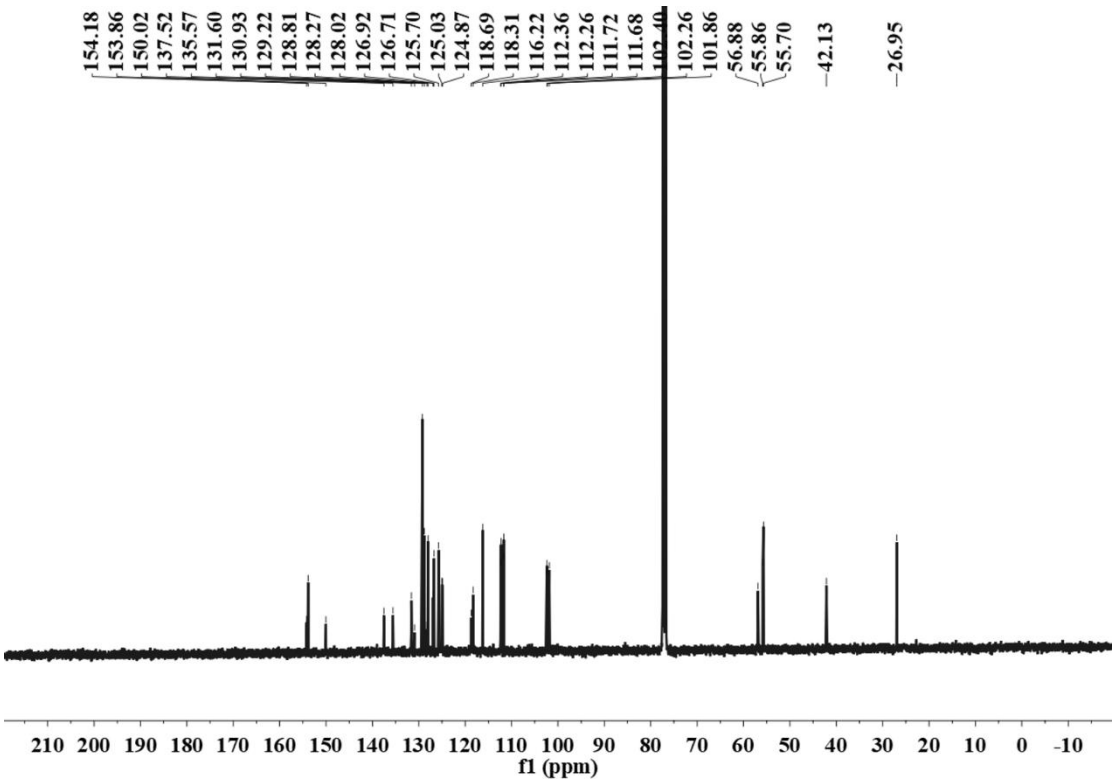

Supplementary Figure 57. ^{13}C NMR spectra of **4i** in $CDCl_3$.

[1] Li Y, Zhang D, Yu Y, et al. A Cascade Strategy Boosting Hydroxyl Radical Generation with Aggregation-Induced Emission Photosensitizers-Albumin Complex for Photodynamic Therapy. *ACS Nano* 2023;17:16993-17003. [DOI: 10.1021/acsnano.3c04256]

[2] Sun L, Yuan Y, Li R, et al. Significantly enhanced photocatalytic performance of In_2O_3 hollow spheres via the coating effect of an N,S-codoped carbon layer. *J Mater Chem A* 2019;7:25423-25432. [DOI: 10.1039/C9TA07891F]

[3] Chen X, Shen X Y, Guan E, et al. A pyridinyl-functionalized tetraphenylethylene fluorogen for specific sensing of trivalent cations. *Chem Commun* 2013;49:1503-1505.[DOI: 10.1039/C2CC38246F]

[4] Lian P, Wang K, Liu H, et al. Reacting Molecular Oxygen with Butanone under Visible Light Irradiation: A General Aerobic Oxidation of Alkenes, Sulfides, Phosphines, and Silanes. *Org Lett* 2023;25:7984-7989.[DOI: 10.1021/acs.orglett.3c03096]

[5] Stepen A J, Bursch M, Grimme S, Stephan D W, Paradies J. Electrophilic Phosphonium Cation-Mediated Phosphane Oxide Reduction Using Oxalyl Chloride and Hydrogen. *Angew Chem Int Ed* 2018;57:15253-15256. [DOI: 10.1002/anie.201809275]

[6] Bugaenko D I, Karchava A V. Electron Donor-Acceptor Complex Initiated Photochemical Phosphorus Arylation with Diaryliodonium Salts toward the Synthesis of Phosphine Oxides. *Adv Synth Catal* 2023;365:1893-1900.[DOI: 10.1002/adsc.202300351]

[7] Chen Q, Zeng J, Yan X,et al. Mild and efficient oxidation of phosphorus(III) compounds with Selectfluor. *Tetrahedron Lett* 2016;57:3379-3381. [DOI: 10.1016/j.tetlet.2016.06.078]

[8] Laye C, Lusseau J, Robert F, Landais Y. The Trityl-Cation Mediated Phosphine Oxides Reduction. *Adv Synth Catal* 2021;363:3035-3043.[DOI: 10.1002/adsc.202100189]

[9] Wu C-J, Zhong J-J, Meng Q-Y, et al. Cobalt-Catalyzed Cross-Dehydrogenative Coupling Reaction in Water by Visible Light. *Org Lett* 2015;17:884-887. [DOI: 10.1021/ol503744a]

[10] Wang Y, Ma C-Q, Li X-L, et al. A novel strategy of constructing an artificial light-harvesting system based on a supramolecular organic framework for photocatalysis. *J Mater Chem A* 2023;11:2627-2633. [DOI: 10.1039/D2TA09227A]